Comunicações Geológicas

Comunicações Geológicas (2020) 107, Especial III, 133-149
ISSN: 0873-948X; **e-ISSN:** 1647-581X

Geochemistry of Iberian Pyrite Belt Portuguese sector massive sulfide deposits-related volcanic rocks. Considerations on hydrothermal alteration, petrology and tectonic evolution

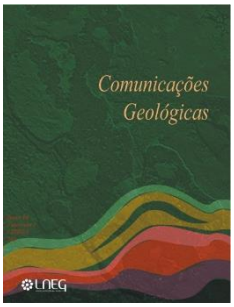

Geoquímica das rochas vulcânicas associadas aos jazigos de sulfuretos maciços do setor português da Faixa Piritosa Ibérica ocidental. Considerações sobre alteração hidrotermal, petrologia e evolução tectónica

I. Morais[1*], L. Albardeiro[1], M. J. Batista[2], J. X. Matos[1], R. Solá[2], D. P. S. de Oliveira[2], R. Salgueiro[2], V. Araújo[3], N. Pacheco[3]

Artigo original
Original article

https://doi.org/10.34637/manf-ad71

Abstract: A geochemical compilation database of the main volcanic units of the Volcano-Sedimentary Complex (VSC) of the Iberian Pyrite Belt (IPB), one of the largest provinces of massive sulfides on a global scale, is presented and discussed. For this purpose, we used several mineral exploration rock geochemistry databases from six IPB areas, namely Cercal, Lagoa Salgada, Lousal, Aljustrel, Neves-Corvo and Chança, regarding unaltered/hydrothermaly altered felsic volcanic units interbedded in the Famennian-Late Visean volcano-sedimentary sequences of the VSC. Volcanic rocks within the Phyllite-Quartzite Formation (Givetian-Famennian) IPB basement were also considered. From this, Neves-Corvo sector rhyolites (Rhyolite type 1 and 2) present the most intense hydrothermal alteration, directly related with the age of mineralization and coeval with hosted VSC sedimentary formations. Similar cases were also observed in the volcanic units hosting Lagoa Salgada, Chança and Aljustrel Volcanic-hosted massive sulfide (VHMS) deposits. The variety of felsic and intermediate volcanic rocks in the IPB (and within each sector) reflect different petrogenetic processes and/or distinct crustal sources. Application of Zr vs TiO_2 binary diagrams allows to define three main trends of andesitic (Lagoa Salgada and Chança sectors), dacitic-rhyodacitic (Aljustrel sector) and rhyolitic (Cercal, Neves-Corvo, Aljustrel and Lousal sectors) composition. Cercal rhyolites are the most evolved felsic rocks ($Zr/TiO_2 \approx 1562$), followed by Neves-Corvo rhyolites ($Zr/TiO_2 \approx 936$), Lousal ($Zr/TiO_2 \approx 845$) and Aljustrel ($Zr/TiO_2 \approx 840$). In addition, four distinct compositional clusters can be distinguished based on Al_2O_3/TiO_2 *vs* Zr/TiO_2 and Al_2O_3/Zr *vs* TiO_2/Zr ratios according to its nature as, rhyolitic, rhyodacitic/dacitic and andesitic, probably reflecting differential partial melting rates. Yb_n *vs* $La/Yb_{(n)}$ diagram ratio indicates that Neves-Corvo (mainly 2 types of rhyolites), Aljustrel (Tufo da Mina rhyolitic unit), as well as Lagoa Salgada sector rhyolites are projected along FIIIa and FIIIb rhyolite fields considered of higher metalliferous potential in the IPB, once their petrogenetic processes are considered ideal to trigger, sustain and host hydrothermal systems and consequently VHMS deposits. Future work, combining geochemical characterization of each volcanic unit with their stratigraphic positioning, is essential in order to achieve a correct correlation between the different sectors and, is therefore, a useful tool in IPB mineral exploration and drill-hole data correlation.

Keywords: Geochemistry, volcanic rocks, tectono-magmatic setting, Iberian Pyrite Belt.

Resumo: Neste trabalho são apresentadas e discutidas as interpretações resultantes de uma compilação de dados geoquímicos das principais unidades vulcânicas do Complexo Vulcano-Sedimentar (CVS) da Faixa Piritosa Ibérica (FPI), uma das maiores províncias de sulfuretos maciços à escala global. Para tal, foram utilizadas várias bases de dados de prospeção mineral relativas a análises químicas de rocha total para seis áreas: Cercal, Lagoa Salgada, Lousal, Aljustrel, Neves-Corvo e Chança (unidades vulcânicas intercaladas nas sequências vulcano-sedimentares de idade Famenniano-Viseano superior do CVS). Foram também considerados dados de rochas vulcânicas nos sedimentos basais da Formação Filito-Quartzítica (Givetiano-Famenniano). Os riólitos tipo 1 e 2 de Neves-Corvo apresentam a alteração hidrotermal mais intensa e estão diretamente relacionados com a idade da mineralização, sendo coevos com as formações sedimentares hospedeiras do CVS. Casos semelhantes são observados nas unidades vulcânicas que alojam os depósitos vulcânicos hospedeiros de sulfuretos maciços (VHMS) de Lagoa Salgada, Chança e Aljustrel. A variedade de rochas vulcânicas félsicas e intermédias na FPI (e dentro de cada setor) deve refletir diferentes processos petrogenéticos e/ou fontes crustais distintas. A aplicação do diagrama binário Zr *vs* TiO_2 permite definir três tendências principais que correspondem aproximadamente às rochas de composição andesítica (setores da Lagoa Salgada e Chança), dacítica-riodacítica (setor de Aljustrel) e riolítica (setores do Cercal, Neves-Corvo, Aljustrel e Lousal). As rochas vulcânicas félsicas mais evoluídas são os riólitos do Cercal ($Zr/TiO_2 \approx 1562$), seguidos dos riólitos de Neves-Corvo ($Zr/TiO_2 \approx 936$), Lousal ($Zr/TiO_2 \approx 845$) e Aljustrel ($Zr/TiO_2 \approx 840$). Além disso, quatro grupos de composições distintas podem ser reconhecidos com base nas razões Al_2O_3/TiO_2 *vs* Zr/TiO_2 e Al_2O_3/Zr *vs* TiO_2/Zr de acordo com a sua natureza, riolítica, riodacítica/dacitica e andesítica, provavelmente refletindo diferentes taxas de fusão parcial. A aplicação do diagrama Yb_n *vs* $La/Yb_{(n)}$ indica que os riólitos do setor de Neves-Corvo (principalmente dois tipos), Aljustrel (unidade riolítica Tufo da Mina) bem como as rochas vulcânicas da Lagoa Salgada são projetadas ao longo do campo dos riólitos do tipo FIIIa e FIIIb, sendo estes considerados os de maior potencial metalífero na FPI, pois os seus processos petrogenéticos são considerados ideais para desencadear, sustentar e hospedar sistemas hidrotermais e, consequentemente, depósitos de VHMS. Pretende-se, no futuro, continuar a desenvolver esta investigação envolvendo a

caracterização geoquímica de cada unidade vulcânica, de acordo com o seu posicionamento estratigráfico, de forma a obter uma correlação sustentada entre os diferentes setores. Esta metodologia é assim uma ferramenta útil em prospeção mineral e na correlação de dados de diferentes sondagens.

Palavras-chave: Geoquímica, rochas vulcânicas, enquadramento tectono-magmático, Faixa Piritosa Ibérica.

[1] Laboratório Nacional de Energia e Geologia (LNEG), Bairro da Vale d´Oca Ap. 14, 7601-909 Aljustrel, Portugal.
[2] Laboratório Nacional de Energia e Geologia (LNEG), Estrada da Portela, Zambujal, Ap. 7586, 2611-901 Amadora, Portugal.
[3] Somincor/Lundin Mining, Stª Bárbara de Padrões, 7780-409 Castro Verde, Portugal.

*Autor correspondente/Corresponding author: igor.morais@lneg.pt

1. Introduction

The Iberian Pyrite Belt (IPB) is one of the largest volcanic/sediment-hosted massive sulphide (VSHMS) provinces including more than 88 known deposits, representing the largest sulfur and iron crustal anomaly on Earth (Laznicka, 1999; Tornos *et al*., 2008). Some of those deposits are considered giant in size, *e.g*., Neves-Corvo, Aljustrel, Lousal and São Domingos (in Portugal) and Rio Tinto, Tharsis, Sotiel and Aznalcóllar (in Spain), comprising ca. 2000 Mt of massive sulfides (Sáez *et al*., 1996, 1999; Leistel *et al*., 1998; Tornos *et al*., 2005; Tornos *et al*., 2008). Identical metallogenetic provinces, such as Val d´Or (Canada) and the Mount Read Belt (Tasmania), are also hosted in a Volcanic-Sedimentary Complex (VSC) sequence as IPB polymetallic mineralizations (Oliveira, 1990; Leistel *et al*., 1998; Carvalho *et al*., 1999; Oliveira *et al*., 2013).

Due to its base metal occurrences, the IPB has been subject of numerous mineral exploration programs in the last decades, which have gathered a huge volume of geological, geochemical and geophysical data. These data sources were attained either through research programs (VolcRosário, IPBVectors, EXPLORA, SmartExploration and GeoFPI) carried out by LNEG or by data acquisition carried out by exploration companies and entities (*e.g*., AGC, Avrupa/Maepa, Azarco, EDM, Empresa Mineira do Cercal, EPOS, IGM, Lundin Mining, Minaport, Northern Lyon, Redcorp, Soc. Mineira Rio Artezia Technical Reports, LNEG Archive database).

The IPB stratigraphic sequence has been defined in key areas as Aljustrel (Schermerhorn, 1971; Barriga *et al*., 1988; Leitão, 2009; Silva *et al*., 1997; Barrie *et al*., 2002; Barrett *et al*., 2008b; Inverno *et al*., 2008), Neves-Corvo (Leca *et al*., 1983; Oliveira *et al*., 2004, 2013; Pereira *et al*., 2008), Lagoa Salgada (Oliveira *et al*., 1997; Matos *et al*., 2000; de Oliveira *et al*., 2011), Caveira and Lousal (Matos and Oliveira, 2003; Matos and Relvas, 2006; Rosa *et al*., 2010; Relvas *et al*., 2012; Matos *et al*., 2014), São Domingos (Webb, 1958; Carvalho, 1971; Oliveira and Matos, 2004; Matos *et al*., 2006) and Pomarão (Boogaard, 1967; Oliveira *et al*., 2007; Albardeiro *et al*., 2020). However, recent regional scale detailed studies have shown that the correlation between stratigraphic sequences in different IPB sectors is sometimes over-estimated, since the sedimentary and volcanic sequences are strongly heterogeneous, and can change drastically in few hundred meters due to lateral and vertical facies variation and tectonic influence (Tornos, 2006; Oliveira *et al*., 2013). High resolution stratigraphic correlations across the entire basin have been made with the biostratigraphic control of the main VSC sedimentary units by palynomorph associations and absolute U-Pb age dating in zircons in the main volcanic units (*e.g*., Pereira *et al*., 2008; Oliveira *et al*., 2004, 2013; Solá *et al*., 2015; Albardeiro *et al*., 2017, 2020).

Besides stratigraphy and geochronology studies, geochemistry strongly contributes for correlation purposes focusing on petrogenetic classifications, hydrothermal alteration and the geotectonic evolution of the IPB. These issues are here presented and discussed based on a whole-rock geochemistry database regarding the most studied areas of the Portuguese sector - Neves-Corvo, Aljustrel, Cercal, Lousal, Lagoa Salgada and Chança. A significant number of samples has been collected over the years in areas/structures affected by intense hydrothermal alteration whereas barren volcanic units are almost not considered in the lithogeochemical sampling programs.

2. Geological setting of Iberian Pyrite Belt

The IPB province is located in the most southwestern sector of the Iberian Peninsula, extending over 230 km long by 20-70 km wide, as the foremost domain of the South Portuguese Zone (SPZ) (Julivert *et al*., 1974; Oliveira, 1990; Oliveira *et al*., 2013, 2019), a tectonostratigraphic terrane sutured to the Iberian Massif during the Variscan Orogeny (Quesada, 1996) (Fig. 1). The province is limited to the north by the Pulo do Lobo Devonian age terrain and overlained by the Late Visean-Moscovian Baixo Alentejo Flysch Group (essentially Mértola and Mira formations).

A localized extensional setting for the genesis of IPB is consensual for most authors. IPB was generated after Devonian distensive tectonic regime (Munhá, 1983; Mitjavila *et al*., 1997; Rosa *et al*., 2006) on a former continental sea causing the establishment of graben-type structures (Oliveira, 1990) and the subsequent settlement of voluminous igneous rocks coexisting with sedimentary deposition engendering a volcano-sedimentary complex hosting VMS deposits. This setting evolved to a compressive regime during Visean times ending with the Variscan collision with Gondwana and the Rheic Ocean closure (Oliveira *et al*., 2019 and references therein). However, a strictly compressional tectonic regime in a continental arc is an alternative model proposed for IPB by Onézime *et al*. (2003).

The IPB stratigraphic succession comprises, from base to upwards: 1) the Phyllite-Quartzite Group (PQ) – a siliciclastic open platform mega-sequence (Oliveira *et al*., 2019) composed of dark shales with intercalations of thin-banded siltstones and quartzites with limestone lenses in its upper section (*Forno da Cal* and *Nascedios* limestone units) (Oliveira, 1983, 1992; Oliveira *et al*., 2004, 2013, 2019; Albardeiro *et al*., 2020; Mendes *et al*., 2020). It is Givetian – latest Famennian (Strunian) in age, given by ammonoids, conodonts and palynomorphs (Boogaard, 1963; Fantinet *et al*., 1976; Cunha and Oliveira, 1989; Oliveira *et al*., 1997; Oliveira *et al*., 2004; Pereira *et al*., 2008; Matos *et al*., 2014); 2) the VSC – divided in Lower and Upper VSC sequences at Neves-Corvo and Lousal-Caveira regions, is represented by Late Famennian age and Late Tournaisian to Late Visean age formations (Oliveira *et al*., 2004, 2013; Pereira *et al*., 2008, 2014; Matos *et al*., 2014). VSC sedimentary rocks are dated as Famennian to Late Visean based on palynomorphs and rare conodonts (Oliveira, 1990; Oliveira *et al*., 1997; Oliveira *et al*., 2004, 2013, 2019; Pereira *et al*., 2008). This Complex comprises several bimodal volcanic rocks, black shales, siltstones, minor quartzwackes, siliceous shales, jaspers and cherts, purple shales and massive sulfides lenses. VSC includes several volcanic episodes (intrusive and extrusive) dominated by felsic rocks (rhyolites, rhyodacites and dacites), coherent facies and monomictic breccias (Rosa *et al*., 2016) and intermediate to mafic rocks (basalts, spillites and minor andesites). The widespread presence of marine fossil content (radiolarian, conodonts and ammonoids) points out to a submarine depositional environment.

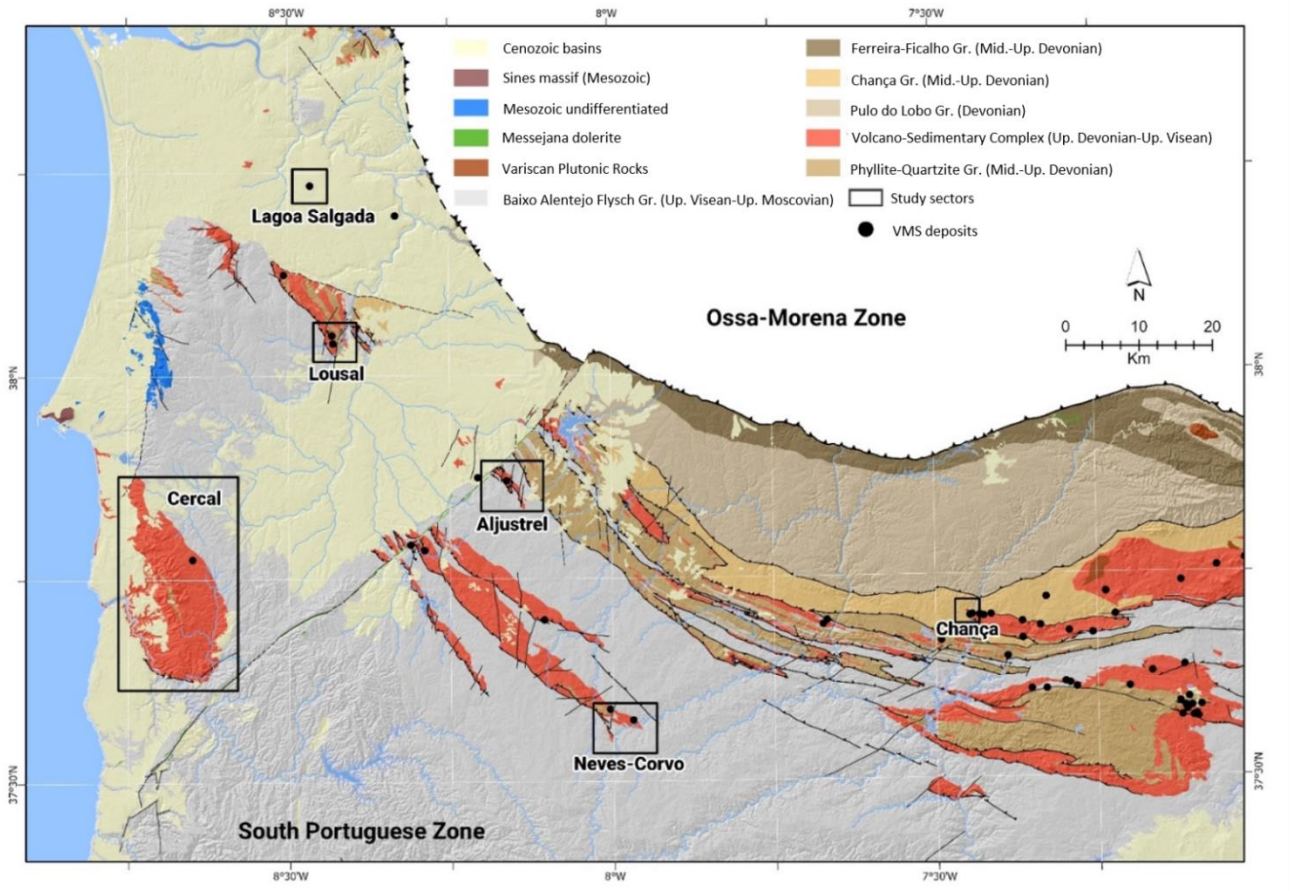

Figure 1. Geological map of South Portuguese Zone with Iberian Pyrite Belt studied sectors (adapted from Oliveira, 1990; Barriga *et al.*, 1998; Leistel *et al.*, 1998; Oliveira *et al.*, 2006).

Figura.1. Mapa geológico da Zona Sul Portuguesa com os setores estudados na Faixa Piritosa Ibérica (adaptado de Oliveira, 1990; Barriga *et al.*, 1998; Leistel *et al.*, 1998; Oliveira *et al.*, 2006).

During Late Strunian, favorable anoxic conditions lead to the development of the giant massive sulfide mineralizations hosted in black shale units. The age of these black shales (Neves Fm. in the Neves-Corvo Mine and Lousal-Caveira Fm. in the Caveira and Lousal mines) associated with interbedded felsic volcanic rocks crossed by mineralized hydrothermal fluids is considered a key mineral exploration horizon, as identified in Neves-Corvo, Lousal-Caveira and Aznalcollar mines (Oliveira *et al.*, 2004, 2013; Pereira *et al*., 2008; Matos *et al*., 2011, 2014); 3) the *Baixo Alentejo* Flysch Group (BAFG), also named as *Culm* in Spain (Schermerhorn, 1971), rests above the VSC, comprising three syn-tectonic formations with age progradation from northeast to southwest, Mértola, Mira and Brejeira Fm (Oliveira, 1990; Oliveira *et al*., 2006, 2013). The former, directly overlying the IPB, consists of a turbiditic sequence embracing alternations of greywacke beds, massive or showing Bouma divisions (Walker, 1979) and dark grey shales, yielding Mid- to Late-Visean age spores (Pereira *et al*., 2008, 2014).

Within the IPB Portuguese sector, the VSC is exposed throughout Variscan aligned (N50W direction) discontinuous structures, showing distinct thickness (up to 1300 m) and geological features (Strauss, 1970; Carvalho, 1976; Routhier *et al*., 1980; Oliveira, 1990; Quesada, 1996; Leistel *et al*., 1998; Sáez *et al*., 1999; Tornos, 2006; Oliveira *et al*., 2013, 2019). The following IPB mineral sectors are hereby described from NW towards SE.

2.1. Key-areas volcanic rocks and sequences

i) Lagoa Salgada sector

Lagoa Salgada orebody is the northern most known IPB deposit recognized to present and occurs underneath 128 m of Alvalade Cenozoic Basin sediments (Oliveira *et al*., 1997; Matos *et al*., 2000; de Oliveira *et al*., 2011). The orebody comprises two geographically distinct zones: a central stockwork and a northwest massive sulfide lens. They include four types of mineralizations: primary massive sulfide, gossan resulting from weathering of the primary mineralization, copper-rich stockwork, and gold-rich silicified zones, which appear to be structurally controlled (de Oliveira *et al*., 2011).

The VSC is characterized by a thick sequence of volcanic rocks while sediments are chert horizon related and PQ Fm. basement has not been, so far, intercepted by exploration drill holes. A Feldspar-quartzphyric Volcanic Unit (FVU) and a Quartzphyric Volcanic Unit (QVU) were identified (Matos *et al*., 2000; de Oliveira *et al*., 2011). The former consists of intermediate to felsic porphyritic volcanic lavas with coarse feldspar-quartz-phyric phenocrysts, locally including coherent facies with porphyritic and auto-breccia textures (monomictic fragments and jigsaw-fit) and fine-grained chlorite-sericite volcanic rocks. Hydrothermal alteration to chlorite-quartz with

disseminated sulfide is intensely close to the massive orebody where footwall replacement textures are common. The QVU comprises felsic porphyritic tuffs with abundant quartz phenocrysts with meter-thick intercalations of volcano-sedimentary breccias. Semi-massive sulfides and stockwork footwall hydrothermal chlorite + pyrophyllite zones were intercepted (DDH LS1) showing extreme volcanic rock leaching (Relvas *et al*., 1994; Matos *et al*., 2000). Berrie *et al*. (2002) dated a footwall dacitic tuff and a hanging wall rhyolitic 356.2 ± 0.7 and 356.4 ± 0.8 Ma respectively.

ii) Lousal-Caveira sector

Lousal Mine is located in NW IPB region (Fig. 1), along a NW-SE VSC trend. Other massive sulfide mineralizations are present in the area: Caveira and Arneirões mines and the Monte da Bela Vista sulfide occurrence are known (Matos and Filipe, 2013). This region comprises, among others, the Lousal, Caveira and São Francisco da Serra anticlines with significant VSC and PQ sequence outcrops (Oliveira *et al*., 2013; Matos *et al*., 2014).

A Lower VSC sequence comprises a thick sequence of rhyolitic lavas (> 300 m) from Famennian age. Outcrop ages of 361 ± 4 Ma (Caveira mine) and 361.8 ± 4 Ma (Monte Bela Vista, Lousal) were obtained (Rosa *et al*., 2009.). According to Rosa *et al*. (2010), the Lousal rhyolites have small coherent cores, locally with flow bands, grading to surrounding massive clastic intervals (hyaloclastite) formed by quenching of original volcanic glass. The clasts show frequent *jigsaw-fit* arrangement, locally perlitic and planar or curviplanar margins. The Lousal-Caveira Fm. (Strunian) black shales were assigned to the LN biozone (Pereira *et al*., 2012; Matos *et al*., 2014). Massive sulfide and stockwork mineralization are hosted by both sediments and felsic volcanic rocks at Lousal and Caveira (Matos *et al*., 2003, 2014, 2015; Matos and Relvas, 2006; Relvas *et al*., 2012), in close proximity with the volcanic centre that may have driven hydrothermal circulation. Mafic volcanic rocks are present with spillitic alteration at Lousal mine open pit. Here, basaltic rocks found at the top of the Upper VSC sequence have abundant autoclastic breccia and pillow lavas.

iii) Cercal sector

The *Cercal* anticline is located in the westernmost sector of the IPB. This structure is NW-SE oriented and corresponds to the most voluminous sequence of VSC outcrops in the Portuguese IPB. The stratigraphic sequence includes, from bottom upwards, the PQ Fm. (Pereira *et al*., 2008), the VSC, and the "*Xistos das Abertas Fm*", which passes gradually to the Mira Fm. flysch sequence (Carvalho, 1976). The VSC is composed by: 1) a Lower Felsic volcanic sequence (also known as A1 volcanism with coherent rhyolites, flows, pyroclastic facies, breccia, agglomerates); 2) an Upper felsic volcanic sequence (A2 proximal volcanism with felsites, volcanic sediments and breccia, and Castelo Volcanic sequence distal volcanism with lavas and volcanic sediments); 3) an Intermediate to mafic sequence (volcaniclastic rocks, lavas and dolerites) and above them, the siliceous shale/volcaniclastic *S. Luis* Fm. These lithologies are interdigitated with the Upper Felsic and the intermediate to mafic volcanic rocks. Particularly in the north-eastern flank, *S. Luis* Fm. and *Castelo* volcanic sequence intercalations has spotted stockwork type mineralization (Salgadinho) and a continuous jasper-like horizon above. A radiometric age range of ca. 374 - 371 Ma for the lower sequence was obtained (Rosa *et al*., 2009) while the S. Luis Fm. basal units brachiopods were ascribed to the Late Strunian (Quiring, 1936). Volcanic rocks of the VSC are then older than Strunian age sediments, meaning that this volcanism is the oldest in the IPB Portuguese sector (Carvalho, 1976).

iv) Aljustrel sector

The massive sulfide deposits in *Aljustrel* are composed by six deposits: Gavião, São João, Moinho, Algares, Estação and Feitais. Only the Feitais and Moinho deposits are currently being mined. The Aljustrel anticline structure is enclosed by the Mértola Fm turbidites and truncated to the NW by the major NE-SW Messejana fault. Beyond this, the Paleozoic formations are buried under 60 to 100 m of Cenozoic clastic and limy sediments of the Alvalade Basin.

The Aljustrel Paleozoic stratigraphic sequence includes the Mértola Fm. (flysch turbiditic shales and greywackes) and the VSC represented by the Paraíso Fm. (siliceous shales, phyllites, volcanogenic sediments, purple shales, jaspers and cherts with mineralizations of Mn), felsic and minor mafic rocks, massive sulfides, jaspers, cherts and Mn horizons. The PQ basement is not recognized. The felsic volcanic sequence was divided according to volcanic facies and lithostratigraphic position in lower and upper units (Schermerhorn *et al*., 1969, 1987; Leitão, 1992, 2009). The former includes "*Tufo com Megacristais*" (Megacrysts volcanic unit), a megacrysts of potassium feldspar dated from 356.5 ± 1.3 Ma by U/Pb (Rosa *et al*., 2009) and a fine-grained felsic facies unit with pyroclastic flows, feldspar tuffs and black shales with siliceous bands, aging 364.2 ± 2 Ma (Rosa *et al*., 2009). The upper volcanic unit comprises two tuff facies with a siliceous matrix "*Tufos da Mina*" and "*Tufos Verdes*", the former dated 352.4 ± 1.9 Ma (Barrie *et al.*, 2002). Barriga and Kerrich (1984) considered that the "*Tufo Megacristais*" and "*Tufos Verdes*" belong to the same formation due to the vertical zonality resulting from hydrothermal alteration.

v) Neves-Corvo mine district

The Neves-Corvo Mine, located at the southeastern termination of the Rosário-Neves-Corvo antiform, contains 7 massive sulfide orebodies (Neves, Corvo, Graça, Lombador, Zambujal, Semblana and Monte Branco).

Stratigraphic succession from the base upwards comprises the IPB full sequence: 1) PQ Fm. pre-orogenic siliciclastic sequence of Givetian to Late Famennian age, and base unknown (Oliveira *et al*., 2004, 2013; Pereira *et al*., 2008; Mendes *et al*., 2018); 2) the Lower VSC sequence comprising bimodal volcanic rocks (felsic rocks and minor basalts), sediments of the Corvo Fm. (Famennian age), black shales and associated massive sulfides of the Neves Fm. (Late Strunian age) and jaspers and carbonates at the top of these sequence (JC unit); 3) the Upper VSC sequence is represented by shales, siltstones, dark shales with nodules and fine-grained volcanogenic rocks, occasional intrusive mafic rocks and minor felsic units; 4) the Mértola Fm. dark grey shales and greywackes.

The ages of Neves-Corvo felsic volcanic rocks have been studied in several research projects being recognized a productive late Famennian volcanic episode at ca. 363 - 357 Ma and a non-productive Tournaisian ca. 353 - 349 Ma episode (Sola *et al*., 2015, 2019; Albardeiro *et al*., 2017).

vi) Chança sector

Chança Mine is located in the northern sector of the IPB, in a VSC lineament that includes also the old mines of Vuelta Falsa, El Carmen, San Fernando, Los Silos, Romanera, El Cura and

Sierrecilla (Spain). The outcropping sulfide mineralization is associated with a VSC rhyolite, an E-W oriented structure (Inverno, 1976; Matos and Rosa, 2001).

Volcanic rocks are formed by porphyritic felsic volcanic lavas, volcanic breccia, locally in contact with sediments developing peperite structures and siliceous shales. The Chança VSC sequence is overlain by the Gafo Fm. (Frasnian age) of the Pulo do Lobo Antiform, formed by shales, greywackes and intrusive volcanic rocks. There is intense hydrothermal alteration marked by chlorite, quartz-sericite and sericite associated with the massive and stockwork sulfides. U/Pb geocronological studies dated the Chança felsic rocks with Tournaisain age: 347.3 ± 6.8 Ma (Solá *et al*., 2019), 349 ± 5 Ma and 354 ± 1 Ma (Rosa *et al*., 2009). The same age is denoted to the Paymogo rhyolites located in the VSC lineament east of the Chança mine: 347.3 ± 0.8 Ma (Donaire *et al*., 2020).

2.2. Previous geochemical studies in IPB

It is widely accepted from previous studies that the IPB magmatism is mainly bimodal, with a predominance of felsic (dacitic to rhyolitic volcanics) over mafic rocks (basalts and dolerites) at current exposure levels (*e.g*., Routhier *et al*., 1980; Munhá, 1983; Mitjavila *et al*., 1997; Soriano, 1997; Leistel *et al*., 1998; Carvalho *et al*., 1999; Thiéblemont *et al*., 1998; Rosa *et al*., 2004, 2006). In opposition, few studies argue that significant amounts of intermediate rock are present (*e.g*., Onézime *et al*., 2003). This circumstance is significant for the volcanism geotectonic classification, once arc settings are typically dominated by intermediate rocks (andesites), while extensional volcanism is generally bimodal. These intermediate "andesitic" compositions in IPB can be apparently reflecting silica and alkali mobility along fractures (Rosa *et al*., 2004) or resulting from felsic crustal derived melts and mafic melts mixture (*e.g*., Mitjavila *et al*., 1997; Codeço *et al*., 2018). This controversy (meaning of "andesitic" composition in IPB) is beyond the scope of this paper and will be discussed elsewhere.

Felsic volcanic rocks belong to a calc-alkaline series ranging from dacites to (high-silica) rhyolites, and their Sr–Nd isotopic composition diversity is interpreted as the result of different degrees of partial melting of upper-crust segments and/or differences in the composition of the source rocks (Mitjavilla *et al*., 1997). Regarding mafic rocks, two main types are distinguished according to Munhá (1983): (1) tholeiitic lavas (transitional to arc tholeiites), which crop out across the whole IPB, and (2) alkaline lavas and dolerites which are similar to recent within-plate basalts, more restricted in the upper part of the VSC volcanic sequence in the Portuguese sector (*e.g*., mafic rocks intrusive in the Late Visean age Grandaços Fm, Neves-Corvo upper VSC). Although basaltic alkaline magmas preserved their within-plate signature, the subalkaline magmas display negative Nb anomalies that make them resemble Volcanic Arc Basalts (VAB). However, these anomalies probably do not reflect a true subduction component, but rather result from assimilation of continental crust (Rosa *et al*., 2004). The existence of alkaline and subakaline affinities may be explained by different degrees of partial melting of a peridotitic mantle (Mitjavila *et al*., 1997), but according to Munhá (1983a, b) at least two different mantle sources are required to explain the compositional differences between the two major basaltic types.

Felsic and mafic volcanic rocks, although closely associated in the IPB, were originated and evolved independently; mafic rocks result from asthenospheric mantle partial melting and their emplacement at shallower (upper-crustal) depths triggering crustal melting and the formation of felsic melts from which the calc-alkaline felsic volcanic suites derive from (Munhá 1983a, b; Mitjavila *et al*., 1997; Thiéblemont *et al*., 1998). Geochemical evidences seem to support a model in which volcanism occurred in an attenuated continental lithosphere setting during a major rifting event, probably triggered by an heat flow supplied by rising mafic magmas (Oliveira *et al*., 2019, and references therein).

For the Rosario–Neves-Corvo antiform (Oliveira *et al*., 2013) the magmatic heat flow should have been comparatively higher than in other sectors of the IPB (*e.g*., Albernoa) where lower temperatures of crustal fusion have been proposed as an explanation for unexpectedly low concentrations of high field strength elements in the felsic volcanic rocks and also the mismatching in apparent andesitic compositions in the geochemical classification diagrams (Rosa *et al*., 2004, 2006).

2.3. Previous studies on volcanic rocks classification (Rosário-Neves-Corvo area)

A geochemical program carried out previously by AGC and Somincor/Lundin Mining allowed to build an extensive database made by major and trace elements of the felsic and mafic units (Barrett, 2008a, unpublished data). From this, an attempt of geochemistry-based genetic classification of the main rhyolite units interpreted in different chemical classes according to its stratigraphic position, from the oldest (Rhyolite type 0) to the youngest (Rhyolite type 6), was made. Subsequent studies (Albardeiro *et al*., 2017) have suggested identical initial crystallization ages between Rhyolite types 1, 2 and 3 (~360 Ma), although Rhyolite type 3 shows a longer age envelope through younger ages (~360 - 350 Ma, Albardeiro *et al*., 2017). Rhyolites types 0 to 4 occur in the lower VSC sequence while Rhyolites types 5 and 6 are scarce and found mainly in the upper sequence. Distal and intra-sedimentary volcanic rocks are located on the upper VSC sequence and will not be considered in this work.

Rhyolite types 0 and 1 are composed by mass flows of volcaniclastic material with fiamme, polymictic and monomictic pumice breccia, quartz feldspar crystal fragments and lithic fragments and rests above the PQ Fm. and bellow Corvo shales being Famennian in age by palynomorph dating (Oliveira *et al*., 2013; Pereira *et al*., 2014). The Rhyolite type 2 shows the same type of facies of Rhyolite type 1. It marks the felsic unit in the footwall of massive sulfide lenses and associated stockwork, and usually presents the most intense hydrothermal alteration halos. This Rhyolite type 2 overlies the Corvo Fm. shales and occurs bellow or within the Late Strunian age black shales from the Neves Fm. that host the massive sulfides. Rhyolite type 3 is mainly a massive volcanic rock, although peperitic and volcaniclastic intercalations are also present interpreted as a cryptodome. This rhyolite occurs generally in the hanging wall of the mineralization and does not superimpose Rhyolites types 1 and 2, suggesting different spatial distribution; it can locally occur immediately below massive sulfides (as defended by Rosa *et al*., 2008), including occasional stockwork veins and chlorite alteration. Rhyolite type 3 occasionally directly overlies the PQ Fm. and can be coeval with footwall Rhyolite type 2 due to the presence of interbedded late Strunian Neves Fm. shales. A subtype of Rhyolite type 3 is detached (Rhyolite type 3'), and commonly located within 10 m of the margins of individual massive rhyolite (Rhyolite type 3), where hyaloclastites also can occur. The Rhyolite type 4 presents a coherent facies and is unmineralized and not known in the mine area but rather in the east, southeast and western sector in the same level as Rhyolite type 3.

The age of the volcanism in Neves-Corvo ranges within ca. 363-349 Ma, divided in an older productive episode (ca. 363-357 Ma) including Rhyolites type 1, 2 and 3, and a younger episode (ca. 353-349 Ma) exclusive of Rhyolite type 3 (Albardeiro *et al*., 2017).

The mafic volcanic rocks present in the Neves-Corvo sector includes both intrusive and extrusive rocks which occur at various levels of the VSC stratigraphic sequence. The extrusive mafic rocks are typicaly intermediate to mafic in composition (Leca *et al*., 1983; Munhá, 1983a) and are represented in Monte Forno da Cal area defining a typically coherent interval with minor clastic zones at their boundaries (Oliveira *et al*., 2013). These mafic volcanic rocks are found at the base of the VSC sequence, immediately above the PQ Fm. and Forno da Cal limestone and it is probably from Late-Famennian age. Strongly altered dolerites with chilled margins occur as intrusive rocks in the Upper VSC sedimentary sequences. Other levels of mafic volcanic rocks are observed in the form of sills infilling PQ Fm shales and quartzites sometimes showing, pyrrhotite-rich gabbroic textures (*e.g*., Algaré and Forno da Cal drill holes, Pereira *et al*., 2014) in the center of the "*Forno da Cal"* sinform structure.

3. Databases and data quality characterization

The felsic, intermediate and mafic volcanic rock analytical data used for this study (Fig. 1, Tab. 1 in Annex) result from geochemical data compilation obtained from several exploration company's programs in the last decades. Both drill hole and outcrop data were selected from representative IPB sectors, such as: i) Cercal (Elf Aquitaine, 1985); ii) Lagoa Salgada (de Oliveira *et al*., 2011; Barrett, 2013; LNEG databases); iii) Aljustrel (Barrett, 2008b); iv) Neves-Corvo (Barrett, 2008a; Somincor/Lundin Mining databases); v) Lousal (AGC-Pirites Alentejanas and LNEG databases) and vi) Chança (AGC and LNEG databases) were used, all included in LNEG lithogeochemical databases.

The primary objective of data acquisition by exploration and mining companies depends intrinsically on the purpose for which they were acquired (usually volcanic structures with hydrothermal halos). Old data adquired by Elf Aquitaine (1985) aimed to characterize for the first time ever the geochemistry the Cercal volcanic units. Barrett (2006) and de Oliveira *et al*. (2011) in Lagoa Salgada, Barrett (2013), in Aljustrel, and Barrett (2008b), together with Somincor/Lundin Mining, in Neves-Corvo, have created geochemical databases used for hydrothermal alteration studies in an attempt to classify chemostratigraphically the main felsic and mafic volcanic units and their relationship with massive sulphides mineralizations.

The analytical methodologies used for data acquisition over the years and compiled in the present work are distinct and variable to what detection limits and confidence data levels is concern (Tab. 2). Not always quality control data is provided by the companies, therefore quality control based in standards and duplicates was only performed in data provided by Lundin, from ACME Lab. The accuracy given by the STD SO-18 standard repeated 24 times in the analysis batch, is high (R < 5%) for all the major (oxides), minor and trace elements except Ta, Sm, Tb where accuracy falls in the interval 5% < R < 10%. The precision related with the same standard was above 5% only for Ni. Seven aliquot blanks were produced along with the routine sample batch and the entire major (oxides), minor and trace elements, except Zr, were bellow detection limit, showing that, contamination is not relevant in pulp preparation. Pulps were analysed two times and the results show no significant differences. Duplicates were made in pulps, as it could be in drill core samples and the result of the biplots sample versus duplicate show very high correlation (> 0.9) between sample and duplicate, in the analysed samples and elements.

The analytical data from Barrett (2013) (Lagoa Salgada), Barrett (2008a) (Neves-Corvo databases) and Chança were performed in ACME Labortories in Vancouver, Canada, using ICP-AES and ICP-MS techniques (package 4A + 4B, plus a metals package), older analytical data such as Elf Aquitaine (1985) was performed using UV emission spectrometry to major and trace elements and specific dosages to Rb, Y, Nb, Zr and P_2O_5.

It is important to underline that geochemical compositions in the IPB are strongly influenced by regional metamorphism and hydrothermal alteration (Munhá, 1983b) as well as by secondary alteration stages related to massive sulphide mineralization, such as chloritization, sericitization and/or silicification (*e.g*., Relvas *et al*., 2006a, b). As mentioned before this geochemical database is a compilation obtained from several exploration company's programs in the last decades. Therefore, available data indicate significant redistribution of several major and trace elements during alteration processes and implications for discussion of magmatic affinities and tectonic setting should be done with caution. In addition, other problems regarding the application of geochemical (and tectonic) classification diagrams using HFSE, were reported for several sectors of IPB. For example, in Albernoa felsic rocks display rhyolitic to apparent andesitic compositions, and the mafic rocks display basaltic to apparent dacitic compositions (Rosa *et al*., 2004).

4. Geochemistry of volcanic rocks

4.1. Geochemistry of hydrothermal alteration

The behavior of some mobile elements and its relationship with the secondary minerals generated during hydrothermal alteration processes, can be evaluated using the alteration box plot developed by Large *et al.* (2001). This box plot is a graphical representation that uses two alteration indexes: the *Ishikawa alteration index* (AI) (Ishikawa *et al*., 1976) proposed to quantify the intensity of sericite and chlorite alteration that occurs in the footwall of VHMS deposits and is defined as: $AI = [100(K_2O+MgO)/(K_2O+MgO+Na_2O+CaO)]$, and the *chlorite-carbonate-pyrite index* (CCPI) developed by Large *et al*. (2001), as: $CCPI = [100(MgO+FeO_{total})/(MgO + FeO_{total} +Na_2O+K_2O)]$. The application of this diagram allows a quick and easy discrimination of the different types and their degrees of hydrothermal alteration affecting the studied volcanic rocks (Fig. 2).

In the Neves-Corvo sector (Fig. 2a), most of the felsic volcanic rock samples are significantly altered by hydrothermal processes associated to the powerful hydrothermal system originating the deposit (Relvas *et al*., 2006, 2014; Morais *et al*., 2019). Following the terminology used for the above mentioned chemostratigraphy classification of volcanic units (Barrett, 2008a, 2012), Rhyolites Type 1 and Type 2 show a more intense hydrothermal alteration related to changes in margins of productive hydrothermal systems (weak sericite alteration – Trend 1), intense sericite – chlorite ± pyrite alteration typical of the proximal footwall alteration (Trend 2) and chlorite ± sericite ± pyrite alteration (Trend 3). These trends agree with the stratigraphic positions of the rhyolite types (Rhyolite type 1 associated with Corvo Fm. and Rhyolite type 2 associated with Neves Fm.) and directly related to above or adjacent massive sulfide mineralization. The Rhyolite type 0, although chemically and stratigraphically related to the Rhyolite type 1 and interpreted as the first phase of volcanism (Barrett, 2014), does not show significant hydrothermal alteration. Most of the Rhyolite types 3

Table 1. Major and trace element concentrations in felsic, intermediate and mafic volcanic rocks from the studied sectors of the Iberian Pyrite Belt. Lithogeochemistry data compiled from: 1) Barrett (2008a) and Somincor/Lundin Mining databases; 2) Elf Aquitaine, 1985; 3) Barrett (2008b); 4) LNEG databases; 5) de Oliveira *et al*. (2011); 6) Barrett (2013). Felsic, intermediate and mafic volcanic rocks classification of Neves-Corvo, Aljustrel and Lagoa Salgada according with Barrett (2008) and Barrett (2013). Samples with hydrothermal alteration were considered.

Tabela 1. Concentrações de elementos maiores e traço nas rochas vulcânicas felsicas, intermédias e máficas dos setores estudados da Faixa Piritosa Ibérica. Dados de litogeoquímica compilados de: 1) Barrett (2008a) e bases de dados da Somincor/Lundin Mining; 2) Elf Aquitaine, 1985; 3) Barrett (2008b); 4) bases de dados do LNEG; 5) de Oliveira *et al*. (2011); 6) Barrett (2013). Classificação das rochas vulcânicas félsicas, intermédias e máficas de Neves-Corvo, Aljustrel e Lagoa Salgada de acordo com Barrett (2008) e Barrett (2013). Foram consideradas amostras com alteração hidrotermal.

		Neves Corvo Felsic Volcanic Rocks						Neves-Corvo Intermediate and Mafic Volcanic Rocks			
		Rhyolite 0 n = 16	Rhyolite 1 n = 136	Rhyolite 2 n = 354	Rhyolite 3 n = 217	Rhyolite 3´ n = 49	Rhyolite 4 n = 43	Associated with Grandaços Fm. n = 19	Associated with PQ Fm. n = 5	Associated with Graça Fm. n = 3	Above PQ Fm. n = 19
SiO_2	%	68.89-84.87	64.46-83.63	54.82-91.27	56.99-90.68	58.75-80.94	65.09-76.76	35.49-47	40.71-52.28	49.89-57.82	24.45-63.37
TiO_2	%	0.07-0.17	0.071-0.34	0.065-0.243	0.056-0.187	0.089-0.2	0.134-0.234	1-2.827	2.157-2.645	0.752-0.892	0.625-0.95
Al_2O_3	%	6.91-15.98	5.77-16.67	5.06-21.04	4.74-20.26	9.24-21.07	11.82-18.01	12.04-19.02	12.96-18.96	17.84-21.63	16.19-21.54
Fe_2O_3	%	1.18-14.47	0.66-16.36	0.45-20.14	0.78-14.7	1.11-8.21	1.63-5.29	6.2-15.01	9.92-29.5	3.04-7.33	3.59-39.26
FeO	%	1.06-13.02	0.594-14.724	0.405-18.122	0.702-13.23	0.999-7.389	1.467-4.76	5.58-13.506	8.93-26.544	2.74-6.6	3.23-35.33
MnO	%	0.01-0.25	0.005-0.21	0.005-0.35	0.005-0.37	0.005-0.12	0.005-0.2	0.11-1.08	0.06-0.17	0.07-0.15	0.06-0.66
MgO	%	0.35-2.93	0.28-3.3	0.04-8.16	0.1-7.7	0.23-4.52	0.31-3.92	2.72-15.55	3.34-8.79	2.71-5.37	1.54-7.32
CaO	%	0.01-1.58	0.006-3.99	0.005-5.6	0.05-3.74	0.25-4.51	0.29-4.21	2.39-9.33	0.63-2.87	2.61-3.65	0.09-11.26
Na_2O	%	0.06-3.05	0.006-4.12	0.005-6.11	0.07-6.19	0.07-4.8	0.12-6.8	0.04-5.81	0.01-3.92	3.29-5.51	0.01-8.05
K_2O	%	0.17-4.74	0.02-5.03	0.03-5.84	0.23-5.96	1.18-5.3	0.54-6.71	0.03-6.11	0.06-2.33	1.36-3.42	0.01-2.93
P_2O_5	%	0.001-0.03	0.0005-0.067	0-0.24	0.002-0.535	0.079-1.135	0.06-0.48	0.12-0.74	0.481-0.98	0.12-0.2	0.03-0.22
Cr_2O_3	%	0.001-0.002	0.001-0.035	0.001-0.017	0.0005-0.005	0.0005-0.006	0.001-0.02	0.006-0.096	0.002-0.006	0.009-0.01	0.004-0.01
Tot. C	%	0.01-1.39	0.01-2.46	0.01-2.68	0.01-2.14	0.01-1.89	0.01-1.74	0.02-3.27	0.02-3.41	0.67-1.36	0.02-2.53
Tot. S	%	0.01-0.49	0.01-3.03	0.01-5.51	0.005-5.49	0.005-5.85	0.01-0.55	0.01-0.4	0.02-3.77	0.02-0.13	0.01-1.6
Cu	ppm	0.4-2506.1	0.6-965	0.8-7362.1	0-843.7	0.8-495.3	2.6-43	15-82	1-3419.4	0-32	0-291
Pb	ppm	0.2-34.8	0.3-650.7	0.4-2285.5	0.6-1025	0.8-202	1.8-65.5	1-21	0-56.9	0-3	0-822
Zn	ppm	12-2831	6-3481	0.5-5856	4-4913	2-199	6-130	57-127	44-310	24-100	40-683
Ba	ppm	49.4-791	4-1360	5-1328	34-1583	144-1175	59-1299	11-531	8-284	142-444	2-612
Ag	ppm	0.05-0.3	0.05-2.2	0.05-7.3	0.05-5.7	0.05-1.2	0.1-0.2	0.05-0.1	0.1-2.5	0.1-0.1	0.05-4.6
Au	ppm	-	-	-	-	-	-	-	-	-	-
As	ppm	0.25-2008	0.25-4068.3	0-4661.1	0-2967	0.25-195.1	0.6-44	0.25-57	10-251.7	1-10	0-74
Sb	ppm	0.01-2.4	0.005-17.2	0-49.7	0-69.8	0.005-9.3	0.005-1.3	0-0.4	0.1-1.3	0.1-0.3	0-0.8
Bi	ppm	0.05-0.6	0.05-13.4	0.05-53	0.05-5.4	0.05-7.5	0.05-0.9	0.05-0.1	0.1-75.8	0.1-0.1	0.05-12.9
Cd	ppm	0.05-9.6	0.05-9.6	0.05-15.4	0.05- 5.5	0.05-0.7	0.1-0.2	0.05-0.2	0.1-0.2	0.1-0.1	0.05-45.1
Hg	ppm	0-3.15	0.005-3.15	0-14.52	0-12.14	0.005-4.12	0-1.34	0-0.1	0-0.18	0-0	0-1.9
Tl	ppm	0.05-0.3	0.05-1.9	0.05-4.4	0.05-12.5	0.05-1.8	0.1-0.6	0.05-0.2	0.1-0.1	0.1-0.1	0.05-0.3
Se	ppm	0.25-3.6	0.25-5.3	0.25-34.5	0.25-14	0.25-6.9	0.5-0.5	0.25-0.5	0.5-21.9	0.5-0.5	0.25-3
V	ppm	4-22	4-46	4-58	2.5-36	4-13	5-16	176-320	77-282	78-139	36-147
Ni	ppm	0.4-20	0.4-131	0.7-67	0.4-26	1.8-33	5-89	22-500	20-30	20-28	10-22
Co	ppm	0.2-16.9	0.4-100.7	0.3-76.2	0-19.8	0.25-19.6	0-4	24-65	19-150.9	14-29	10-41
Sc	ppm	3-9	3-28	1-12	3-16	7-17	3-10	18-46	10-37	18-22	13-23
Rb	ppm	6.2-221.4	0.7-192	1.4-254	8.5-283	42-170.6	23-286	1-220	2.4-102	57-113	13-143
Sr	ppm	6.9-73.4	2.2-81.6	2.4-435	15-523.3	21.8-221	26.6-251	50-606	13.2-131	94-130	2-325
Cs	ppm	0.9-15.6	0.2-7.6	0.1-10	0.6-16.8	2.1-14	1.1-11.1	0.4-9.7	0.4-4.3	4.3-5.5	0.4-5.4
Sn	ppm	3-110	2-177	0.5-120	1-68	3 - 54	3-9	1-4	2- 05	1-1	0.5-206
W	ppm	0.25-2.3	0.25-18.5	0.1-18.6	0.25-20.5	0.7-5.8	0.5-2.9	0.2-13.7	0.7-26.9	0.6-2.3	0.25-8.7
Mo	ppm	0.05-3.6	0.05-6	0.05-26.6	0.05-30.4	0.05-2.4	0.1-5	0.2-3.2	0.8-2.6	0.1-0.2	0.1-2.6
Ga	ppm	11.9-25	10.8-27.9	4.4-29.3	8.2-35.7	12.9-32.1	15.5-39.6	14.3-25.5	19.5-33.3	16.5-21.3	16.3-31
Be	ppm	0.5-3	0.5-6	0.5-6	0.5-7	0.5-8	1-7	0.5-2	0.5-0.5	0-0	0.5-0.5
U	ppm	2.4-5.2	1.7-5.9	0.2-13.4	0.5-11.6	0.3-26.3	2.1-8.3	0.1-2.3	1.6-3.4	0.4-0.7	0.2-1.2
Hf	ppm	4.4-11.6	4.8-14.2	1.5-6.4	1.5-6.4	3-7.4	4.8-8.3	2.5-6	4.8-7.4	2.8-3.5	2.6-4.1
Ta	ppm	0.7-1.6	0.5-1.9	0.1-1.3	0.3- .8	0.6-1.4	0.8-1.8	0.2-4.2	0.6-5.7	0.2-0.3	0.1-0.6
Th	ppm	7.4-17.1	6.4-18.3	5.8-27	3.1-18	6-16.8	14.3-25.7	0.4-5.6	2.7-7.9	1.3-2.3	1.6-3.6
Nb	ppm	5.6-23.8	7.1-24.2	3-13.5	4.1-21.3	9.8-20.3	12-21.3	2.9-69.5	10.5-98.8	3.8-5.9	3.7-7.8
Y	ppm	36.6-72.4	32.2-101	16.2-66.8	5.5-53.8	27.9-57.8	21-41.3	20-41.9	25.9-64.	12.1-16	9.3-19.3
r	ppm	138.2-314.5	164.3-506.9	44.7-180.5	38.9-183.4	87.8-198.2	147.2-246.1	101.8-308.5	218.6-350.4	105.3-114.9	90-146.5
La	ppm	20.8-51.8	19.1-78.5	7.6-46.8	5.1-39.2	14.6-43.7	28.7-74.5	3.6-43.8	13.5-57.7	5.8-10.5	7.5-15
Ce	ppm	44.8-107.4	43.9-174.4	16.8-95.6	14.2-95.6	32.2-96.3	76.5-162.1	10.2-96.2	36.7-119.3	16.1-22.6	19.2-34.7
Pr	ppm	5.6-13.42	5.58-21.16	1.96-11.91	1.86-11.29	4.53-12.33	9.37-18.94	1.77-9.92	4.94-12.64	2.32-2.83	2.09-4.02
Nd	ppm	22.6-58.6	21.6-82.9	7.3-42.2	8.1-46	18.7-50	38.9-75.1	8.8-37.7	23.5-49.2	10.6-11.7	8.8-16.8
Sm	ppm	4.07-11.61	4.6-18.28	2.01-9.78	2.09-12.9	5.96-13.56	10.28-15.7	2.74-7.41	5.79-8.93	2.19-2.72	1.96-3.76
Eu	ppm	0.36-1.53	0.49-3.39	0.24-1.57	0.26-2.07	0.62-1.86	0.91-1.75	0.8-2.28	1.49-3.12	0.52-0.92	0.47-1.54
Gd	ppm	4.03-12.04	4.81-17.12	2.29-9.58	1.71-12.18	5.84-14.44	8.76-14.06	3.77-7.25	5.43-9.98	2.02-3.05	1.67-3.7
Tb	ppm	0.81-1.99	0.8-2.92	0.45-1.68	0.25-1.98	1.04-2.32	1.19-1.98	0.58-1.21	0.91-1.87	0.35-0.48	0.31-0.63
Dy	ppm	5.34-12.26	5.03-18.25	2.9-11.44	1.27-11.18	5.54-12.9	5.36-9.03	3.72-6.98	4.97-11.52	2.15-2.69	1.71-3.49
Ho	ppm	1.18-2.53	1.19-3.72	0.57-2.15	0.23-1.78	0.91-2.15	0.67-1.38	0.71-1.52	0.97-2.47	0.46-0.56	0.34-0.71
Er	ppm	3.85-7.5	3.6-10.92	1.72-6.81	0.56-4.93	2.45-5.58	1.31-3.22	1.93-4.45	2.71-7.46	1.34-1.65	1.07-1.92
Tm	ppm	0.59-1.16	0.54-1.59	0.27-1.03	0.09-0.75	0.32-0.76	0.16-0.42	0.28-0.65	0.39-1.12	0.2-0.24	0.14-0.26
Yb	ppm	3.66-7.46	3.27-10.87	1.68-6.29	0.55-4.11	1.72-4.51	0.89-2.47	1.67-4.19	2.56-7.12	1.33-1.37	1.08-1.75
Lu	ppm	0.6-1.12	0.58-1.57	0.23-0.87	0.08-0.61	0.25-0.64	0.11-0.36	0.26-0.63	0.37-1.06	0.2-0.21	0.15-0.26
Source		1)	1)	1)	1)	1)	1)	1)	1)	1)	1)

Table 1 (cont.)

Tabela 1 (cont.)

	Cercal		Aljustrel felsic vlcanic rocks				Lousal			Chança		Lagoa Salgada
	Felsic n = 97	Mafic n = 14	Megacristais n = 23	Rhyolite A n = 7	Rhyolite B n = 6	Mina Tuff n = 10	Rhyolites n = 12	Andesite n = 4	Basalts n = 4	Rhyolites n = 5	Andesites n = 31	Intermediate rocks n = 229
SiO_2	66.7-89.7	34.7-52.6	56.39-73.08	72.15-77.87	71.11-82.12	66.4-78.1	48.48-72.54	44.99-58.65	35.82-45.83	72.35-76.72	20.7-65.45	24.58-76.75
TiO_2	0.07-0.63	0.58- .85	0.435-0.761	0.133-0.175	0.049-0.271	0.15-0.33	0.104-0.508	0.82-0.923	1.179-2.175	0.144-0.239	0.149-0.934	0.16-1.209
Al_2O_3	5.7-17.4	6.6-16.4	13.4-23.63	11.3-14.52	3.06-15.31	9.34-17.7	4.98-24.52	17.67-20.6	10.42-16.26	9.84-11.1	5.34-17.68	5.16-25.74
Fe_2O_3	0.3-9.9	10.9-16.3	3.08-6.01	1.54-2.19	1.56-9.22	1.23-5.52	2.11-30.07	4.68-7.29	10.11-13.5	2.74-4.64	5.06-31.75	0-22.44
FeO	0.1-7.8	7.4-11.6	2.77-5.41	1.386-1.971	1.404-8.298	1.11-4.97	1.90-27.06	4.21-6.56	9.10-12.15	2.47-4.18	4.55-28.569	0.35-20.196
MnO	0.04-2.15	0.18-0.3	0.02-0.22	0.02-0.05	0.02-0.07	0.09-0.09	0.03-0.1	0.04-0.15	0.16-0.3	0.04-0.09	0.02-0.35	0.002-0.81
MgO	0.1-3.2	1.6-25.7	0.53-5.39	0.6-2.08	0.3-1.85	0.49-5.27	0.49-4.93	3.81-5.51	7.41-20.16	2.73-4.84	0.48-13.81	0.02-16.12
CaO	0.1-3.7	2.2-11.7	0.28- 1.83	0.26-1.62	0.06-0.5	0.02-4.09	0.02-2.43	3.6-8.3	4.35-7.92	0.05-0.55	0.03-7.36	0.02-10.08
Na_2O	0.1-5.9	0.1-6.5	1.08-6.27	1.26-7.39	0.1-7.52	0.16-4.92	0-7.42	0.1 8-5.76	0.01-3.92	0.04-0.09	0-4.72	0.01-6.33
K_2O	0.1-10.4	0.1-1.3	0.33-6.89	0.08-4.03	0.06-4.91	0.44-4.44	0.03-3.76	1-4.38	0.33-0.82	1.76-2.91	0.05-5.39	0.005-6.23
P_2O_5	110-2430	-	0.08-0.38	0.02-0.03	0.01-0.07	0.04-0.11	0.008-0.395	0.117-0.158	0.163-0.638	0.019-0.037	0.017-0.417	0.02-0.261
Cr_2O_3	-	57-1220	0.002-56	10-19	10-27	-	0.002-0.003	0.01-0.011	0.028-0.151	0.002-0.006	0.003-0.065	0.001-0.067
Tot. C	-	-	0.02-0.17	-	-	-	0.06-0.7	0.21-1.76	0.31-1.97	0.01-0.22	0.01-1.27	-
Tot. S	-	-	0.04-0.25	-	-	-	0.03-15.65	0.02-0.02	0.04-0.06	0.93-2.54	0.02-21.53	0.01-13.3
Cu	6-777	13-119	0.2-242	33-72	16-105	1-15	6.5-7133	2.8-48.5	47.4-123.5	2.7-117.5	0.6-3487.1	1-6501
Pb	12-432	19-205	1.4-76.4	12-28	2- 20	3-46	2.5-565.3	1.4-16.8	1.1-19.4	4.1-111	1.3-108.7	2-6211
Zn	11-567	82-158	45-120	51-122	17-137	25-140	59-835	40-73	59-125	29-1017	16-169	11-7350
Ba	29-1405	23-246	171-708	-	-	168-659	5-572	169-284	5-298	269.2-399.7	2.1-2347.4	4-1208
Ag	-	-	0-0	-	-	-	0.3-4	-	0.4-0.4	0.1-2.1	0.1-1	0.1-22.7
Au	-	-	0.5-15	-	-	-	1.3-119	1.5-1.5	-	3.9-114.8	0.5-66.2	0.0002 - 237.8
As	-	-	0.7-11.8	-	-	2-190	0.8-661	0.6-16.9	3.1-5.3	15.6-73	0.5-275.2	1-7400
Sb	-	-	0.1-1.1	-	-	0.4-29	0.3-12.2	0.1-0.3	0.1-0.2	0.2-11.5	0.1-6.8	0.1-1000
Bi	-	-	0.1-0.5	-	-	-	0.1-62.6	-	-	0.5-4.1	0.1-34.8	0.1-46.5
Cd	-	-	0.1-0.3	-	-	1-2	0.1-1.8	-	0.2-0.2	0.1-2.9	0.1-0.2	0.1-124.8
Hg	-	-	0.01-0.14	-	-	-	0.03-1.12	-	0.01-0.05	0.05-0.77	0.01-7.65	0-39.6
Tl	-	-	0.1-0.8	-	-	-	0.1-9.2	-	-	0.1-0.3	0.1-8.9	0.1-25
Se	-	-	0.5-0.7	-	-	-	0.5-25.6	-	6.8-6.8	0.6-3.9	0.5-59.9	0.5-39.4
V	-	-	30-56	5-16	5-32	2-20	10-40	104-148	164-217	8-19	58-209	20-355
Ni	11-455	12-101	8-41	2-6	2-16	2-9	25-25	41-49	109-734	5-20	5-237	5-154
Co	-	39-1141	5.1-35	13-34	14-29	1-4	0.9-500.7	18.6-20.9	39.1-88.6	1.4-3	10-60.2	3-39
Sc	-	-	10.6-17	-	-	3.4-10.8	3-26	16-18	21-25	7-9	7-35	2-32
Rb	20-270	15-30	9-223	3-255	2-233	23-278	1.1-165.5	30.9-125.5	0.7-17.8	68.6-126.2	0.7-131.2	1-300
Sr	12-274	73-700	79-346	86-143	57-200	25-470	1.3-311.9	119.7-521.4	27.2-503	5-13.4	1.9-217.9	3-525
Cs	-	-	4.5-14	-	-	2-26	0.2-8.2	3.7-5.9	0.6-2.1	2.2-4.4	0.5-9	0-28
Sn	-	-	0.5-10	-	-	-	4-93	-	1-1	9-18	1-25	1-213
W	-	-	0.8-81.3	-	-	-	0.6-9	1.4-1.4	0.5-0.8	0.9-2.2	0.5-8.6	0.1-21.1
Mo	6-45	-	0.1-1.8	-	-	-	0.3-4.8	0.4-0.4	0.5-2.2	0.9-1.8	0.1-12.7	0.1-4.4
Ga	9-51	19-50	20.5-33.9	-	-	-	9.5-27.2	19-21.1	12.7-19.5	10.5-15.3	7.5-19.1	11-54
Be	-	-	5-5	-	-	2-6	-	-	-	1-1	1-2	5-6
U	-	-	0.8-8.5	1-1	1-4	2.5-4.7	0.8-4.6	0.3-0.9	0.5-1.7	2.1-2.4	0.4-19.2	1-14.4
Hf	-	-	6.5-12.2	-	-	3.1-9.7	2.9- 5	3.6-3.9	1.9-5.1	4.1-5.5	0.8-4.4	1.2-5.5
Ta	-	-	1-1.8	-	-	1-1	0.3-1.5	0.3-0.4	0.8-4.3	0.4-0.6	0.1-0.6	0.2-1.3
Th	-	-	9-22.4	6-12	8-18	7.7-20	3.8-19.5	2.2-2.7	1.3-5.6	8-11.1	1.1-7	1.7-14.3
Nb	3.6-238	0.3-78	13-25.2	8.8-11	6.5-9	12-27	4-19.1	4.5-5.4	14.1-72.6	5.5-7	1.4-7.8	2.5-21
Y	18-680	8-38	30.8-64.9	52-77	47-75.1	34-92	13.9-58.8	12.6-13.8	12.6-23.5	26.7-32.2	5.4-55.5	10-46.5
Zr	50-525	65-320	237-406.2	195-272	53-312	81-318	78.5-513.5	127.4-135.9	84.6-214.7	135.7-169.8	24.7-152	39-209.7
La	21-246	36-115	36.1-65.2	-	-	17.4-44	-	-	-	-	-	5.8-43.5
Ce	-	-	80-141.6	-	-	38-97	-	-	-	-	-	13.1-93.3
Pr	-	-	10.7-18.64	-	-	-	-	-	-	-	-	1.6-10
Nd	-	-	34-68.4	-	-	16-39	-	-	-	-	-	6-37.8
Sm	-	-	6.5-14.15	-	-	3.4-7.9	7.7-38.7	7.9-10.3	8.1-41.4	21.2-28.5	2.2-27.6	1.4-7.7
Eu	-	-	1.2-2.3	-	-	0.3-0.7	20.7-90.4	20.6-23.8	17.6-78.5	45.4-62.4	5.1-62.6	0.4-2.1
Gd	-	-	8.51-13.31	-	-	-	2.83-11.01	2.6-3.22	2.33-9.35	5.56-6.96	0.72-7.54	1.4-6.9
Tb	-	-	1-2.24	-	-	0.8-1.9	11.3-43.8	11.4-13.4	10.8-35.7	19.5-25.8	2.7-30.7	0.3-1.3
Dy	-	-	6.9-12.37	-	0-0	-	2.63-9.76	2.56-2.84	2.6-6.14	4.04-5.13	0.67-6.49	2-7.7
Ho	-	-	1.3-2.27	-	0-0	-	0.39-1.79	0.93-1.01	0.81-1.97	0.42-0.8	0.18-1.4	0.4-1.6
Er	-	-	3.6-6.06	-	0-0	-	2.81-10.71	2.64-2.72	2.78-5.54	3.73-4.89	0.75-7.37	1.2-5.2
Tm	-	-	0.5-0.91	-	0-0	-	0.43-1.66	0.35-0.37	0.47-0.7	0.73-0.91	0.16-1.27	0.2-0.8
Yb	-	-	2.6-5.32	-	0-0	3.5-5.9	3.07-11.18	2.31-2.47	2.76-4.52	4.07-5.57	0.85-7.97	1.19-4.4
Lu	-	-	0.39-0.76	-	0-0	0.5-0.88	0.41-2.24	0.45-0.5	0.51-0.87	0.77-1.12	0.17-1.65	0.19-0.8
Source	2)	2)	3)	3)	3)	3)	4)	4)	4)	4)	4)	4) 5) 6)

samples and subtype 3´ plot within the least altered field of the alteration box plot (Fig. 2a) and may indicate more distal alteration phenomena in relation to the main mineralizing volcanic centers. The few Rhyolite type 4 samples do not present significant hydrothermal alteration, so it is assumed that this may be a post main mineralization stage volcanic event (Albardeiro *et al*., 2017). Most of the intermediate to mafic volcanic rocks do not present significant hydrothermal alteration, although locally it can be intense (sericite-chlorite-pyrite trend) and associated with andesitic rocks and stockworks from the top of PQ Fm. (*e.g*., Algaré Sector; Fig. 2b).

Table 2. Whole rock databases compilations used by sector and reference to the elements analysed and analytical techniques.

Tabela 2. Compilação das bases de dados de rocha total usadas e por setor com referência aos elementos analisados e técnicas analíticas.

IPB studied sectors	Databases (references)	Number of samples	Analysed elements	Analytical techniques
Neves-Corvo	Barrett., 2008a and Somincor/Lundin Mining databases	861	1	ICP-AES and ICP-MS
Cercal	Elf Aquitaine., 1985	111	2	UV emission spectrometry and specific dosage
Aljustrel	Barrett *et al*., 2008b	46	1 and Au	ICP-AES and ICP-MS
Lousal-Caveira	LNEG databases	20	1 and Au except Ce, Pr, Nd and Sm	ICP-AES and ICP-MS
Chança	LNEG databases	36	1 and Au except Ce, Pr, Nd and Sm	ICP-AES and ICP-MS
Lagoa Salgada	LNEG databases de Oliveira *et al*., 2011 Barrett., 2013	229	1 and Au	ICP-AES and ICP-MS

1 – SiO_2, TiO_2, Al_2O_3, Fe_2O_3, FeO, MnO, MgO, CaO, Na_2O, K_2O, P_2O_5, Cr_2O_3, C, S, Cu, Pb, Zn, Ba, Ag, As, Sb, Bi, Cd, Hg, Tl, Se, V, Ni, Co, Sc, Rb, Sr, Cs, Sn, W, Mo, Ga, Be, U, Hf, Ta, Th, Nb, Y, Zr, La, Ce, Pr, Nd, Sm Eu, Gd, Tb, Dy, Ho, Er, Tm, Yb, Lu.

2 – SiO_2, TiO_2, Al_2O_3, Fe_2O_3, FeO, MnO, MgO, CaO, Na_2O, K_2O, P_2O_5, Cu, Pb, Zn, Ba, Ni, Rb, Sr, Mo, Ga, Nb, Y, Zr, La.

In Cercal and Aljustrel sectors (Fig. 2c) most of the samples plot within the least altered field. However, some samples of both areas show a weak diagenetic alteration in the field of albite-chlorite (Trend 7; Fig. 2c), typical of the interaction with sea water at low temperatures (*e.g*., spilites and keratophyres) (Hughes, 1973). Part of the felsic volcanic rocks in the Cercal sector show a K feldspar- sericite alteration (Trend 6; Fig. 2c) that can be develop locally in footwall volcanic rocks (Paulick *et al*., 2001) and probably associated with Salgadinho sulphide deposit. In Lagoa Salgada, chloritization and sericitization processes can be observed in most samples (de Oliveira *et al*., 2011) plotting in the sericite, chlorite and pyrite trends and interpreted by a typical footwall alteration (Large *et al*., 2001). Some samples plot within the least altered field being related with lateral distal facies of the Feldspar-quartzphyric Volcanic Unit (FVU). These are less affected by extreme hydrothermal alteration halo defined at Lagoa Salgada, with the extreme condition defined by the presence of pyrophyllite (Relvas *et al*., 1994; Matos *et al*., 2000). In the Lousal and Cercal areas, the mafic rocks are poorly affected by hydrothermal alteration. In both scenarios the felsic volcanic rocks show similar alterations to those observed in the Lagoa Salgada FVU like rocks with intermediate to felsic composition and associated with stockwork mineralization (*e.g*., Chança pyritic stockwork).

4.2. Whole rock geochemistry

The classification diagram based on the immobile elements, Nb/Y *vs* Zr/TiO_2 (Winchester and Floyd, 1977) (Fig. 3) show several compositios main in subalkaline field. However, a significant group of mafic compositions plot also in the in alkaline field.In the Neves-Corvo sector, most of the samples plot in rhyolite field but a substantial sample set is projected in the rhyodacites, Although the intermediate composition volcanism is considered irrelevant in the Portuguese IPB compared to felsic and mafic volcanic rocks. Figure 3 shows it is quite abundant in sectors like Lagoa Salgada and Chança related to massive sulfide mineralization + stockworks (Lagoa Salgada and Chança VMS mineralization). andesites and alkaline basalt fields, related to intrusive volcanic rocks in the metasedimentary sequences (PQ Fm. and Grandaços Fm.), that may be justified with the ideias expressed in Rosa *et al*. (2004) or resulting from the mixture between felsic crustal derived melts and mafic melts (*e.g*., Mitjavila *et al*., 1997; Codeço *et al*., 2018).

In the Aljustrel, Lousal and Chança areas, most of the rocks have an essentially rhyodacitic-dacitic composition, although in the last two sectors some samples have an andesitic composition but are clearly related to the mineralization.

The felsic volcanic rocks of the Cercal sector have essentially a rhyolitic composition, and the high SiO_2 (> 80%) and low MgO and TiO_2 contents in some samples are indicative of high degree of magmatic fractionation (Thieblemont *et al*., 1998).

The Zr *vs* TiO_2 (Fig. 4) and Al_2O_3 *vs* Zr (Fig. 5) graph shows the elementary concentration distributions obtained for the various sets of studied volcanic rocks. The lines that correlate the various sets of samples represent different igneous precursors, lesser differentiated as bigger the line inclination (wide distribution of TiO_2 in samples and almost no Zr, such as the Chança example). The immobility of these elements has been used and confirmed by detailed studies in the IPB in previous works (Barrett *et al*., 2008a; EPOS, 2014; Rosa *et al*., 2004; Rosa *et al*., 2006; Codeço, 2015).

A simple analysis of the graph Zr *vs* TiO_2 (Fig. 4) allows us to define three main trends in the studied sectors (*y1*, *y2* and *y3*) corresponding roughly to the rocks of andesitic composition (Lagoa Salgada and Chança sectors - *y1*), dacitic-rhyodacitic (Aljustrel sector - *y2*) and rhyolitic (Cercal, Neves Corvo, part of Aljustrel and Lousal sectors - *y3*). The most evolved felsic rocks are the rhyolites of the Cercal with Zr/TiO_2 ratios ≈ 1562, Neves-Corvo Zr/TiO_2 ratios ≈ 936, Lousal Zr/TiO_2 ratios ≈ 845 and Aljustrel Zr/TiO_2 ratios ≈ 840 (Fig. 4). It is noteworthy that of all the rhyolites, those of the Cercal sector are derived from more evolved magmas (higher Zr/TiO_2) coinciding also with the oldest IPB felsic volcanic rocks with ca. 374 - 370 Ma (Rosa *et al*., 2009) and probably related to the first manifestations of known felsic volcanism (Carvalho, 1976). In the Aljustrel sector, the Megacristais Volcanic Unit Zr/TiO_2 ratios ≈ 576 is slightly less evolved than the remaining rhyolites (Rhyolite A, Rhyolite B and Mina tuff) with Zr/TiO_2 ratios ≈ 1159 (Fig. 6). This Megacristais volcanic unit (355 ± 2 Ma, Rosa *et al*., 2009) is younger than the

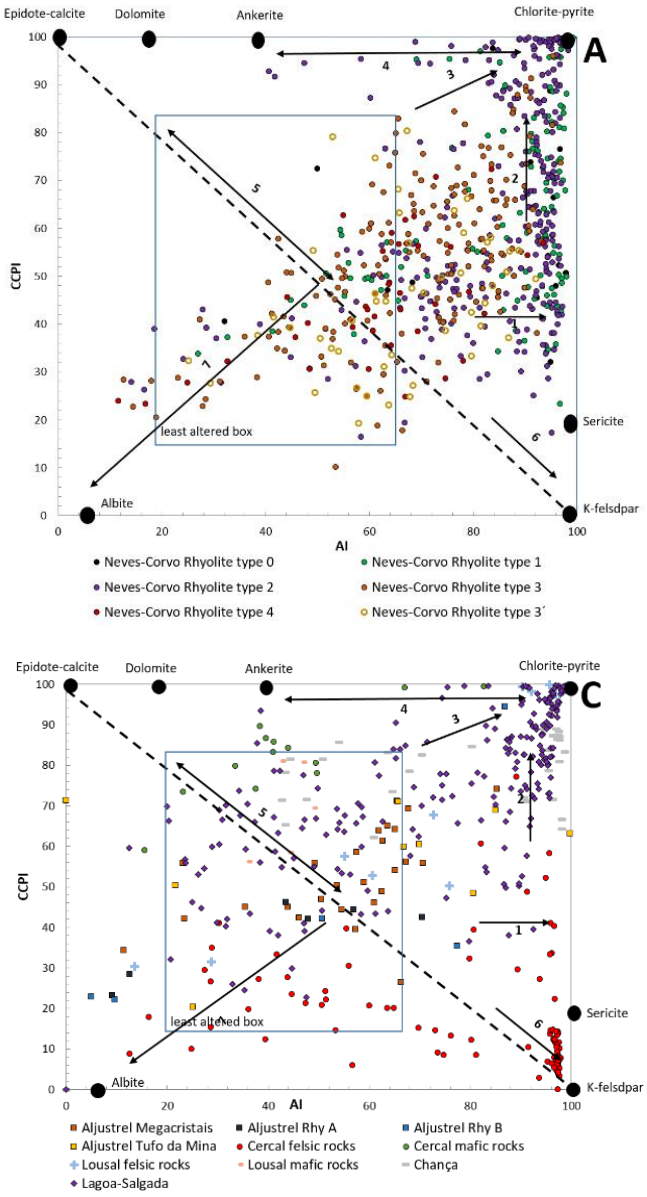

Figure 2. Alteration box plots with the Hashimoto alteration index (AI) (Ishikawa *et al*., 1976) *versus* the chlorite-carbonate-pyrite index (CCPI) (CCPI and diagram from Large *et al*., 2001). Arrows show six common trends during hydrothermal alteration: (1) sericite; (2) sericite-chlorite-pyrite; (3) chlorite-pyrite-(sericite); (4) chlorite-carbonates; (5) carbonates-sericite; (6) K-feldspar. A) felsic rocks of Neves-Corvo sector by rhyolite typology; B) mafic rocks of Neves-Corvo sector; C) volcanic rocks of Cercal, Aljustrel, Lousal, Chança and Lagoa Salgada. MVR – Mafic Volcanic Rocks; VSC – Vulcano-sedimentary Complex.

Figura.2. Gráficos de alteração com o índice de alteração de Hashimoto (AI) (Ishikawa *et al*., 1976) *versus* o índice de clorite-carbonato-pirite (CCPI) (CCPI e diagrama de Large *et al*., 2001). As setas mostram seis tendências comuns durante a alteração hidrotermal: (1) sericite; (2) sericite-clorite-pirite; (3) clorite-pirite-(sericite); (4) clorite-carbonatos; (5) carbonatos-sericite; (6) feldspato K. A) Rochas félsicas do setor de Neves-Corvo por tipologia de riólitos; B) rochas máficas do setor de Neves-Corvo; C) rochas vulcânicas do Cercal, Aljustrel, Lousal, Chança e Lagoa Salgada. MVR – Rochas Vulcânicas Máficas; VSC – Complexo Vulcano-sedimentar.

remaining rhyolites and intrusive rocks in the sequence (Dawson *et al*., 2001). The volcanic rocks of the Lagoa Salgada and Chança sectors, with essentially andesitic composition, derive from less evolved magmas with 207 > Zr/TiO_2 ratios < 260.

Regarding the Neves-Corvo sector, through the projection of the different types of rhyolites (Barrett, 2004, 2008a) in the Al_2O_3 *vs* Zr graph (Fig. 5), it is possible to define four distinctive compositional groups (α1, α2, α3, α4) probably refleting differential partial melting rates. The rhyolitic rocks defined by α1 (Rhyolite type 0 and 1) are the ones that show the most evolved terms, gradually changing to less evolved volcanic units and with less silica content along the α2 and α4 trend (Rhyolite type 2 and 3, 3´). The rhyolite type 4 (defined by α3 trend line) shows a more evolved signature in relation to Rhyolite type 2 and 3 and probably corresponds to a more recent and evolved volcanic event and not related with the mineralizing event.

Despite the dispersion caused by fractionation trends, covariation between element pairs in each rock type can be used to broadly discriminate the rock types based on their element ratio like Al_2O_3/TiO_2 *vs* Zr/TiO_2 and Al_2O_3/Zr *vs* TiO_2/Zr (Figs. 6 and 7) identifying different groups capable of integrating different igneous precursors. Both diagrams clearly show a grouping of the samples into four distinct clusters (β1, β2, β3, β4) according to its nature, rhyolitic, rhyodacitic/dacitic and andesitic. The rocks that make up the Lagoa Salgada and Chança sector, with an essentially andesitic composition, are distributed mainly in the field β1 (Figs. 6 and 7) where the values of Al_2O_3/TiO_2 and Zr/TiO_2 ratios are low.

A second group β2, includes all the volcanic rocks of Aljustrel (except Rhyolite A) and some samples of Chança and Lousal rhyolites with a facies of a rhyolitic nature being the samples of Megacristais Volcanic Unit those that present a high TiO_2/Zr ratio.

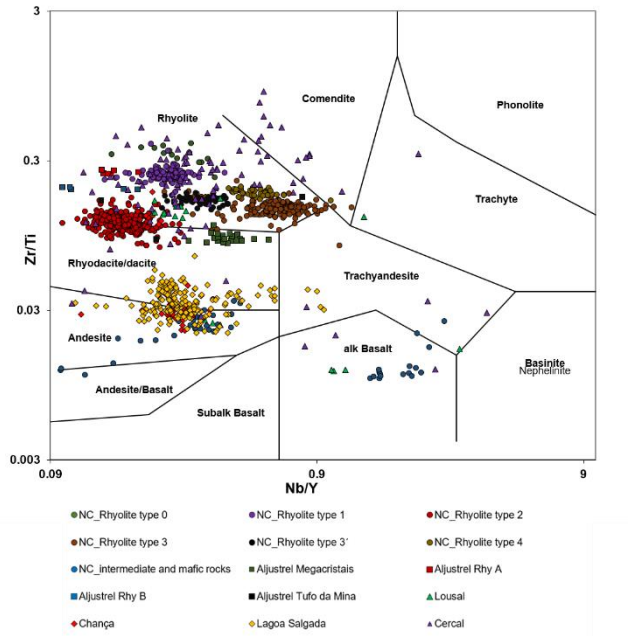

Figure 3. Projection of the samples in Zr/TiO_2 *versus* Nb/Y diagram, with fields by Winchester and Floyd (1977).

Figura 3. Projeção das amostras no diagrama Zr/TiO_2 *versus* Nb/Y nos campos de Winchester and Floyd (1977).

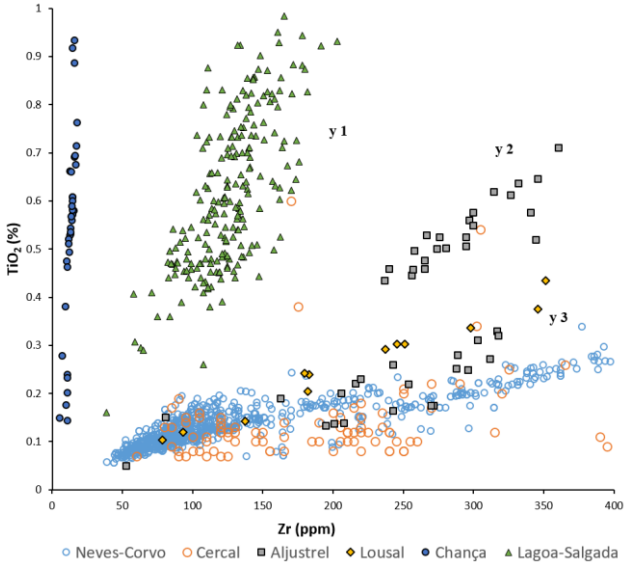

Figure 4. Zr *vs* TiO_2 plot of intermediate and felsic volcanic rocks discriminating the rocks of andesitic composition (*y1)* and more evolved rocks, dacitic-rhyodacitic (*y2*) and rhyolitic composition (*y3*).

Figura 4. Projeção das rochas félsicas e intermédias no gráfico Zr *vs* TiO_2 discriminando rochas com composição andesitica (*y1)* e rochas mais evoluídas, de composição dacítica-riodacítica (*y2*) e riolítica (*y3*).

A third group of samples (β3) is materialized by Neves-Corvo Rhyolite types 2, 3 and 3' with high Al_2O_3/TiO_2 and Al_2O_3/Zr ratios. The last group of samples (β4) is formed by the Rhyolite types 0 and 1 of Neves-Corvo and Rhyolite A of Aljustrel and represent the first manifestations of felsic volcanism known for these sectors (Neves-Corvo and Aljustrel, respectively) characterized by high Zr/TiO_2 and low Al_2O_3/Zr and TiO_2/Zr ratios. The Cercal samples, although showing a heterogeneous geochemical behavior, are largely defined by low TiO_2/Zr ratios similar to the remain rhyolites in other sectors.

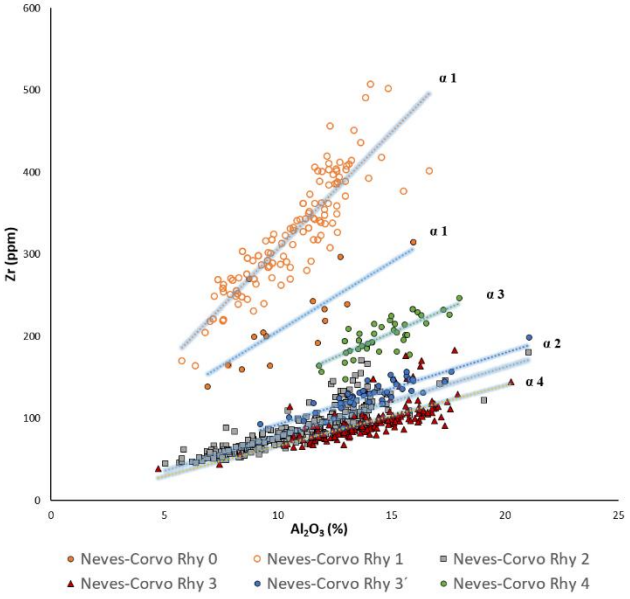

Figure 5. Al_2O_3 *vs* Zr plot of rhyolites types in the Neves-Corvo sector. Classification of types of rhyolites according to Barrett (2004, 2008a). Compositional groups (α1, α2, α3, α4).

Figura 5. Gráfico Al_2O_3 vs Zr dos diferentes tipos de riólitos do setor de Neves-Corvo. Classificação dos tipos de riólitos de acordo com Barrett (2004, 2008a). Grupos composicionais (α1, α2, α3, α4).

The normalized concentration patterns for the minor and trace elements relative to the primitive mantle (Palme *et al*., 2012) of intermediate and felsic volcanic rocks of the studied sectors allow to clearly distinguish two groups (Fig. 8).

The rhyolitic rocks of Aljustrel and Neves-Corvo (except the Rhyolite subtype 3) show negative anomalies in Nb, Ti, Sc and Eu and positive anomalies in Pb and Ba. For the felsic volcanic rocks, the systematic negative anomalies in Nb (Fig. 8A) are typical in rift-related settings where the underlying crust is continental. The negative anomaly in Ti is common in rocks with high content of Si and justified by the presence of titanite in the crystallization residue. The VHMS deposits rich in Pb justify the strong positive anomaly in this element in some samples (except the Rhyolite type 3) as well as the Ba anomaly characteristic of top hydrothermal alteration and variable according to the distance to the ore deposit or active volcanic center. The Lousal and Chança felsic volcanic rocks are depleted in Ti, Al and Sc and enriched in Eu, Tb, Pb and Ba (Fig. 8A).

Typical basaltic rocks show sub-horizontal normalized concentration patterns which are generally characterized by relative enrichment and also depletion (usually of low amplitude) either in incompatible or compatible elements (Fig. 8B).

For the basaltic rocks of Neves-Corvo sector, intrusive in the PQ and Grandaços Fms, two distinct trends are observed: i) enrichment in Nb and slightly in Zr and depletion in Sc; and ii) depletion in Nb, Al and Sc (sometimes in Eu and Ti) and enrichment in Zr. Such a distinction may suggest the existence of two distinct mafic episodes with unknown age to date (probably Visean in age) and associated with different geological processes suggested by both Nb positive and negative anomalies. The presence of two distint trends in mafic rocks is a commun feature within IPB (see section 2.2). The negative Nb anomalies could be explained by assimilation of continental crust rather than a subduction component (*e.g.*, Rosa *et al*., 2004). The intermediate composition rocks of the Neves-Corvo sector (andesitic rocks above the PQ Fm. and correlated with the spillitic rocks of the

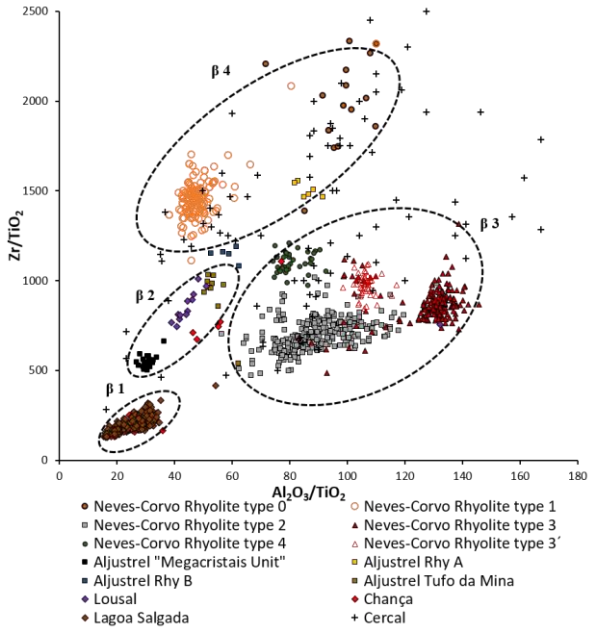

Figure 6. Al_2O_3/TiO_2 vs Zr/TiO_2 plot of intermediate and felsic volcanic rocks of the studied IPB sectors. β1 andesite composition; β2 and β3 rhyodacite/dacitic composition and β4 rhyolitic composition. (Rhy- rhyolite).

Figura 6. Gráfico Al_2O_3/TiO_2 *vs* Zr/TiO_2 das rochas vulcânicas intermédias e félsicas dos setores estudados da FPI. β1 composição andesítica; β2 e β3 composição riodacitíca/dacitíca e β4 composição riolítica. (Rhy- riólito).

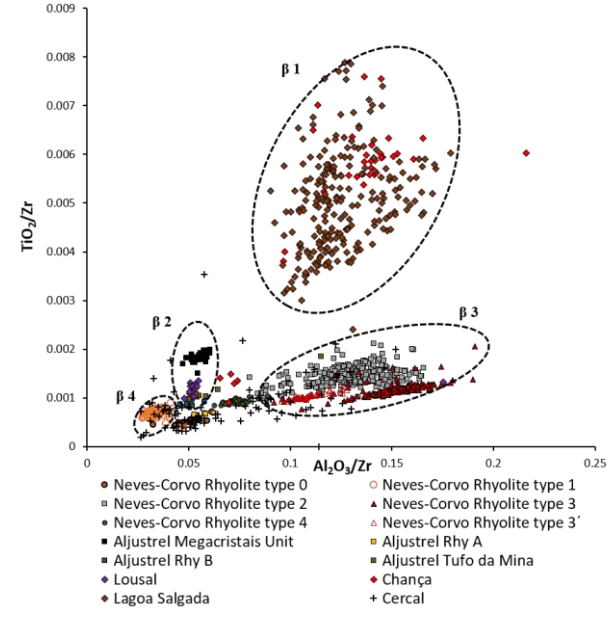

Figure 7. Al_2O_3/Zr *vs* TiO_2/Zr plot of volcanic rocks of the studied sectors. β1 andesite composition; β2 and β3 rhyodacite/dacitic composition and β4 rhyolitic composition.

Figura 7. Gráfico Al_2O_3/Zr *vs* TiO_2/Zr das rochas vulcânicas dos setores estudados. β1 composição andesítica; β2 e β3 composição riodacitíca/dacitíca e β4 composição riolítica.

Forno da Cal and the andesitic rocks of Upper VSC Graça Fm.) have similar normalized concentrations patterns depleted in Nb, Sm, Eu and Sc and slightly enriched in Zr, Hf and Al (Fig. 8C).

The remaining intermediate composition rocks (Lousal, Chança and Lagoa Salgada) are defined by two different trends: i) intermediate rocks of Lousal and Chança extremely enriched in Eu and Tb and depleted in Sc, Ti and Al (only in Chança) (Fig. 8A); ii) intermediate rocks of Lagoa Salgada depleted in Nb, Ti and Sc, suggesting a strong crustal component in these rocks (Fig. 8D).

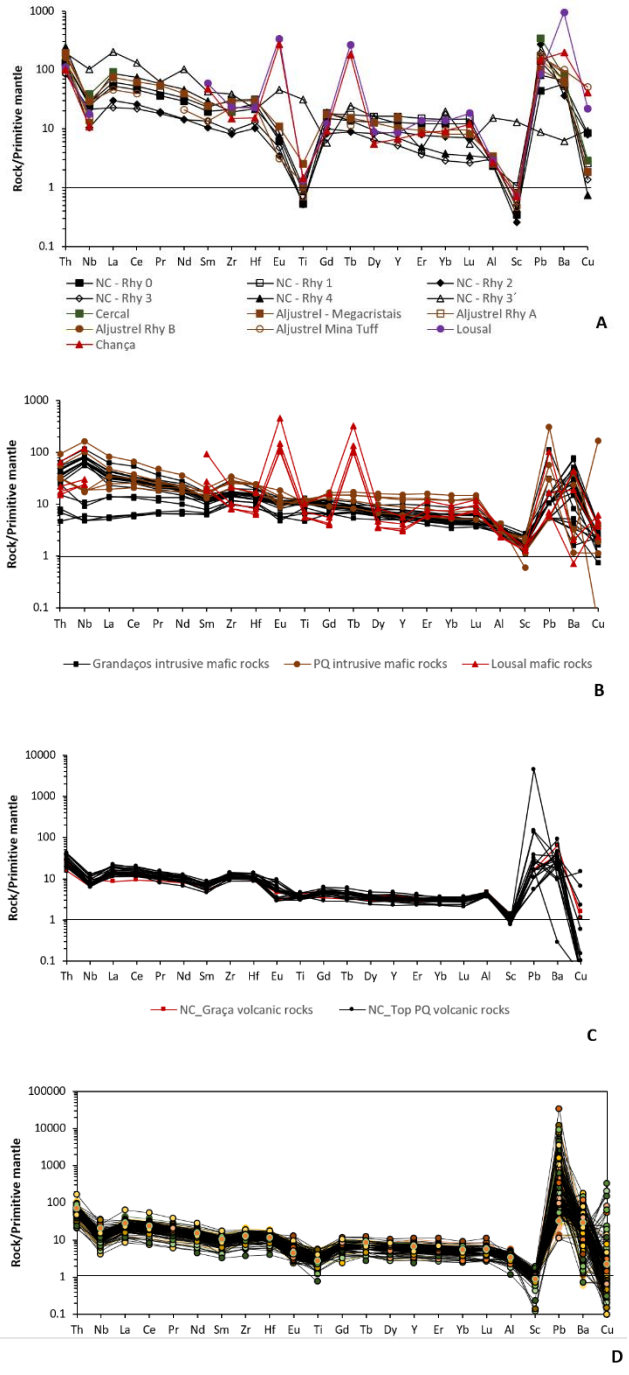

Figure 8. Normalized concentration patterns of major and trace elements (relative to primitive mantle; normalizing values from Palme *et al.*, 2012) of the samples from the various IPB sectors studied. A) felsic volcanic rocks; B) intrusive mafic volcanic rocks of Neves-Corvo; C) intermediate volcanic rocks in the Graça Fm. and top of PQ Fm. (Neves-Corvo area); D) intermediate rocks of Lagoa Salgada.

Figura 8. Padrões de concentração normalizados dos elementos maiores e traço (relativos ao manto primitivo; Valores de normalização de Palme *et al.*, 2012) das amostras dos diversos setores da FPI estudados. A) rochas vulcânicas félsicas; B) rochas vulcânicas máficas intrusivas em Neves-Corvo; C) rochas vulcânicas intermédias na Fm. da Graça e no topo da Fm. PQ (área de Neves-Corvo); D) rochas intermédias da Lagoa Salgada.

4.3. Geotectonic discriminant diagram

Geotectonic diagrams were applied only for mafic (and intermediate rocks), compositions that better reflect the geodynamic environment.

The elements used for tectonic discrimination of mafic and intermediate volcanic rocks must have an immobile behavior during the hydrothermal alteration processes, however, for these studies it is important to use samples that have the smallest hydrothermal alteration. For this interpretation were selected samples projected in the least alteration box plot from Hashimoto alteration índex (AI) versus the chlorite-carbonate-pyrite index (CCPI) (Fig. 2).

Mafic volcanism appears to be less abundant than felsic (and intermediate) in some IPB areas. Mafic volcanism is dominated by basaltic dykes or small veins, intrusive all over the known sequence, and by sometimes extensive local domains of lava flows, even with occasional pillow lavas (Munhá, 1983; Almodóvar *et al*., 1998). In Portugal, some areas like Caveira East, São Pedro das Cabeças and Casével show important VSC sequences with mafic volcanic rocks (Oliveira *et al*., 1992, 2013). The stratigraphic position of the different types of mafic rocks is well defined, i.e., in the base of the VSC and in the Upper VSC sequence (*e.g*., Caveira and Caveira East, Matos *et al*., 2015; Dias *et al*., 2016; and São Pedro das Cabeças). However, their age is not yet constrained in detail, which leads to discussions about its importance in the genesis and metallogenesis of massive sulfide mineralizations.

The Ti-Zr-Y diagram (Pearce and Cann, 1973) is most often used to differentiate the intraplate basalts (WPB) from those generated in divergent and convergent plate margin (MORB and VAB respectively). The Nb-Zr-Y diagram (Meschede, 1986) is similar to the previous diagram although it can discriminate between normal and enriched (or transitional) MORB as mentioned before.

For the mafic volcanic rocks of Neves-Corvo (PQ Fm. and Grandaços Fm.) and Lousal (shales of the upper VSC) regions, the diagrams Hf-Th-Ta (Fig. 9; Wood, 1980) and Ti-Zr-Y (Fig. 10; Pearce and Cann, 1973) show two distinct groups of intrusive mafic volcanic rocks. A first group shows alkaline affinities (typical in OIB – Oceanic Island Basalts) and is projected in the WPB field and a second group, with a calc-alkaline affinity, is mainly projected in the fields associated to an island arc environment.Pearce (2008) used the Th/Yb *vs* Nb/Yb diagram as a proxy for crustal contamination, with crust-contaminated basalts plotting in oblique arrays above the modern MORB-OIB array (Fig. 11).

It is possible to infer that intermediate composition rocks from sectors like Lagoa Salgada and Chança should have resulted from partial mantle melting processes and were incorporated from the lower young crust during their crustal ascension.

At local scale the VSC mafic rocks that occur immediately above the PQ Fm. and probably the first manifestation of volcanism in the IPB (*e.g*., Forno da Cal spillites), are more primitive, but also appear to contain some degrees of crustal contamination, probably related to the incorporation of crustal material from this formation throughout its ascencion.

4.4. Distribution of volcanism and relation with VHMS deposits

Overall, in the IPB bimodal magmatism five temporal major volcanic episodes have been assumed: i) initial felsic volcanism; ii) mafic volcanism; iii) intermedium felsic volcanism; iv) superior felsic volcanism; and v) superior mafic volcanism (Oliveira, 1990; Oliveira *et al*., 2013). However, intermediate

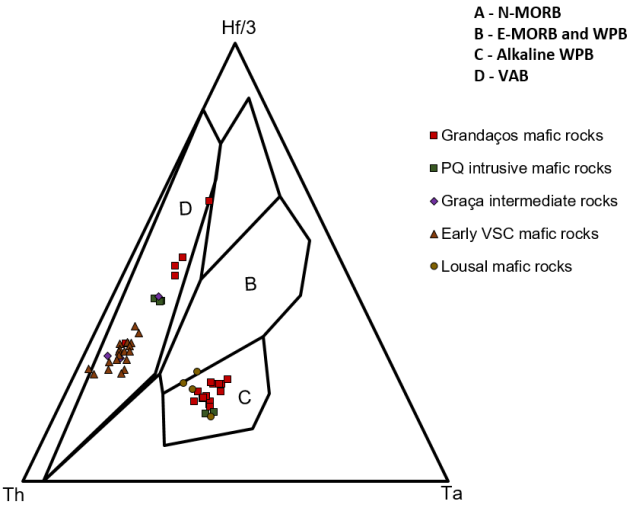

Figure 9. Th-Hf-Ta diagram of Wood (1980) for the mafic rocks of the IPB studied sectors.

Figura 9. Diagrama Th-Hf-Ta de Wood (1980) para as rochas máficas dos setores estudados da FPI.

rocks (andesites), in some cases (Lagoa Salgada and Chança sectors) associated with massive sulfide mineralizations, prevail at the regional and local scales. Recent drill holes to depths more than 2000 m in the Neves-Corvo sector have evidenced the presence of large intrusive mafic rock packages (sometimes more than 100 m thick)., which suggest that mafic volcanism may be locally more important than the felsic one. In fact, regional geological mapping shows these scenarios in areas like Montinho, Caveira East, São Pedro das Cabeças, Casével and Foupana (Odeleite exploration drill holes), mainly associated with Upper VSC sequences of Late Visean age.

The geochemistry of felsic rocks associated with favorable environments of VHMS deposits genesis is strongly dependent on the type of underlying juvenile crust or evolved and this also varies as a function of age (Piercey, 2011). Felsic volcanic rocks located in favorable VHMS environments, like IPB are associated with the partial melting of upper continental crust or continental crust-derived sedimentary rock) origin (Piercey, 2009). These are fundamentally different from those associated with partial melting of a mafic igneous substrate, leading to different signatures of rhyolites associated with different VHMS deposits environments (Piercey, 2009).

Hart *et al*. (2004) proposed a classification based on the Yb_n *versus* $La/Yb_{(n)}$ (n chondrite normalization) ratio can be used to discriminate felsic volcanic rocks associated with VHMS and consequently with high potential to host this type of mineralizations (Fig. 12). According to the used terminology (FI, FII, FIIIa, FIIIb and FIV), rocks projected along the field FIIIa and FIIIb commonly host the major VHMS deposits and their petrogenetic processes, in terms of heat source, considered more favourable to trigger and sustain hydrothermal circulation and mineralization processes (Lesher *et al*., 1986). The FIIIa rhyolites described by Hart *et al*. (2004) have variable negative Eu anomalies, low Zr/Y, and intermediate abundances of HFSE. FIIIb rhyolites exhibit pronounced negative Eu anomalies, low Zr/Y, and high abundances of HFSE, Neves-Corvo Rhyolite type 1 is projected along the field FIIIb. Samples of Rhyolites type 0 and 2 in the Neves-Corvo sector and Lagoa Salgada intermediate rocks project in the field FIIIa and samples of Rhyolite Tufo da Mina in the Aljustrel.

Assuming the petrogenetic model for the formation of FIII felsic volcanic rocks by partial melting at progressively shallower crustal depths in a rift environment, combined with the high thermal flow allows the crustal fusion of low pressure and high temperature within a zone of high volcanic permeability (*e.g.*, pumice breccias).

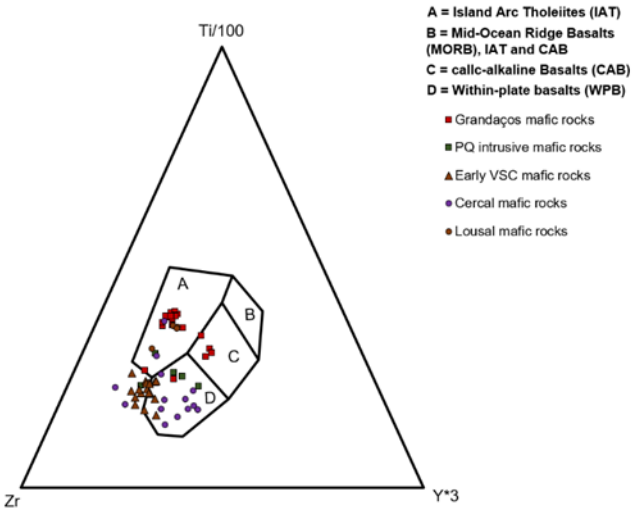

Figure 10. Pearce and Cann (1973) diagram with geotectonic classification of the mafic rocks of the studied sectors.

Figura 10. Diagrama Pearce e Cann (1973) com a classificação geotectónica das rochas vulcânicas máficas dos setores estudados.

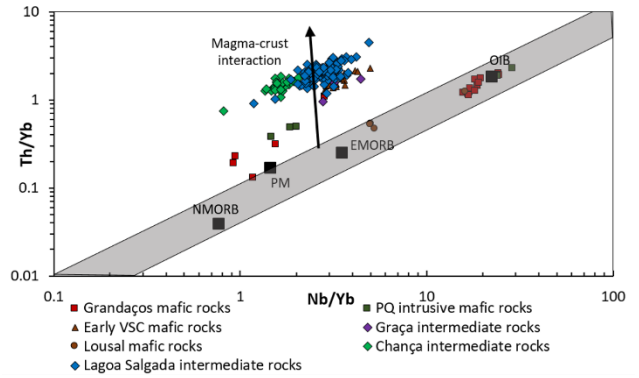

Figure 11. Nb/Yb vs Th/Yb of the studied samples (after Pearce and Peate, 1995). Average N-MORB, E-MORB, PM and OIB compositions from Sun and McDonough (1989).

Figura 11. Gráfico Nb/Yb *vs* Th/Yb das amostras estudadas (depois de Pearce e Peate, 1995). Composição média N-MORB, E-MORB, PM e OIB de Sun e McDonough (1989).

This setting could be favorable to promote the convective flux of mineralizing fluids through these rhyolites and other host rocks and consequently the formation of massive sulfide deposits. Correlating the stratigraphic position of these felsic volcanic rocks (both hosting the VHMS mineralization in Neves-Corvo and Aljustrel) within the favorable geological time window of 358.8-359.8 Ma for the NC Rhyolite type 1 (Albardeiro *et al.*, 2017; Pereira *et al.*, 2020 in press) and 352.4 Ma for the Aljustrel Rhyolite Tufo da Mina (Barrie *et al.*, 2002) (latest Famennian, Strunian, to Middle Tournaisian) will therefore indicate once again the metallogenetic potential of this type of rocks in the context of the IPB mineral exploration. However, some of the samples of the studied sectors such as the Rhyolite types 3 and 4 for Neves-Corvo and Rhyolite Tufo Megacristais in Aljustrel are projected in the field FII of the felsic rocks which may correspond to samples collected in volcanic centers formed after the main mineralization stage and consequently barren or less favorable (example of this is the Rhyolite type 4 from Cotovio-SE Neves-Corvo with 345 - 350 Ma (D. Rosa, Pers. Com.) and Megacristais Volcanic Unit with 352.4-356.6 Ma (Barrie *et al.*, 2002; Rosa *et al.*, 2009) that may have been formed below the maximum depth of the convective fluid (Hart *et al.*, 2004).

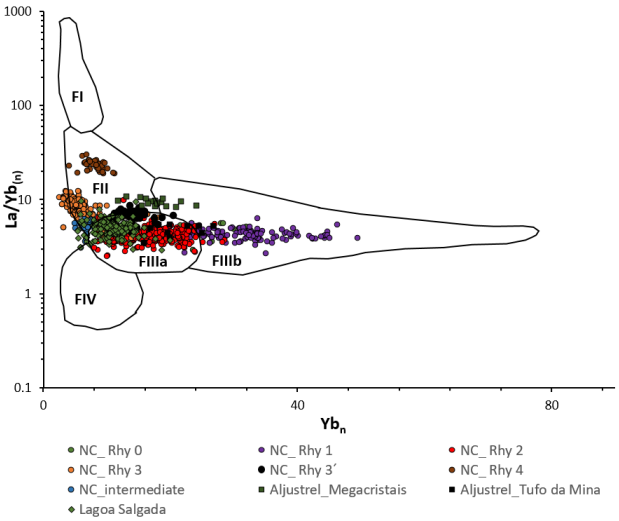

Figure 12. Diagram Yb_n *vs* $(La/Yb)_n$ by Hart *et al.* (2004) for felsic volcanic rocks of the studied IPB sectors. Condrite normalization.

Figura 12. Diagramas Yb_n *vs* $(La/Yb)_n$ de Hart *et al.* (2004) das rochas vulcânicas félsicas dos setores estudados da FPI. Normalização ao condrito.

5. Conclusions

A geochemical compilation of the main volcanic units was conducted in the geological formations of the Volcano-Sedimentary Complex (VSC) from the Portuguese sector of the IPB. For this purpose, were used several existing rock geochemistry databases for six areas Cercal, Lagoa Salgada, Lousal, Aljustrel, Neves-Corvo and Chança.

The general architecture of the IPB corresponds to a huge depression with asymmetric descent of different tectonic blocks that not only influenced the posterior tectonic evolution of the entire belt, but also conditioned the deposition and the location of the main volcanic axis. The depositional record in the IPB is therefore marked by a strong lateral and vertical variation of facies, thus hampering the differentiation and correlation of main lithostratigraphic units inter and intra sectors. Much of these relationships are based on age dating of the foremost sedimentary and volcanic units supported by palynological and geochronological data. Thus, there is a need to harmonize the existent chemostratigrafic scale to the various sectors of the IPB as a complement to a lithostratigraphic scale in order to be a useful tool in mineral exploration of productive volcanic centers.

The hydrothermal alteration of volcanic rocks is one of the most important tools used in mineral exploration, therefore. The presence or absence of hydrothermal alteration in different degrees is an indicator of the presence of hydrothermal fluids that may have driven important metal content. Through the application of the box-plot alteration index Ishikawa alteration index (AI) *versus* chlorite-carbonate-pyrite index (CCPI) it was possible to indicate the likely proximity to a productive volcanic center of the samples of the Neves Corvo (Rhyolite type 1 and 2),

Lagoa Salgada (felsic rocks projecting in alteration trends towards the chlorite-pyrite) and Cercal (felsic rocks into the sericite fields) regarding higher alteration. In the Neves-Corvo sector, where the litho-stratigraphy of volcanic rocks is better defined, four types of volcanic rocks with rhyolitic composition were considered. Given its stratigraphic position, the Rhyolites type 1 and 2 are respectively associated with Corvo Fm. and Neves Fm, and coeval with massive sulfide mineralizations, being those that present a greater degree of hydrothermal alteration. In turn, the Rhyolite types 3 and 3', show less intense hydrothermal alteration indicating greater distance from hydrothermal source, while the Rhyolite type 4 in general does not present alteration. Similar results are observed in the felsic and intermediate volcanic rocks from Lagoa Salgada, Lousal, Aljustrel and Chança far from the hydrothermal event areas.

The IPB geochemical database presented here updates the composition of IPB volcanism, with predominance of felsic over mafic volcanism and with clusters between basalts, basalts-andesites and dacites-rhyolites as described in previous works. However, through deep mineral exploration programs *(e.g.*, Neves-Corvo and Sesmarias exploration project, Alvalade Cenozoic Basin) we may find that mafic volcanism can be more abundant than previously assumed.

The ratio between Yb_n *versus* $La/Yb_{(n)}$ indicates that felsic volcanic rocks projected along FIIIa and FIIIb fields have a greater metalliferous potential. The rhyolitic rocks type 1 and 2 (and some of type 0) (in the Neves-Corvo sector) and Tufo da Mina rhyolitic unit (in the Aljustrel sector) show that they have a greater potential. Their stratigraphic position in relation to massive sulfide mineralization is the same, besides the differences in their ages 358.8-359.8 Ma for Neves-Corvo sector (Albardeiro *et al*., 2017) and 352.4 Ma for Aljustrel sector (Barrie *et al*., 2002). Lagoa Salgada rhyolites also have plot inside FIIIa field.

Geochemical characterization of each volcanic unit combined with their stratigraphic positioning is essential in order to achieve a correct correlation between the different sectors and is therefore a useful tool in mineral exploration.

Aknowledgements

Parts of this study were undertaken in project EXPLORA – Definition of new geological, geophysical and geochemical knowledge vectors applied to Neves-Corvo northern region, Op ALT20-03-0145-FEDER-000025, funded by Alentejo 2020, Portugal 2020 and European Union (ERDF), in association with Somincor-Lundin Mining and Hercules Laboratory of Évora University. We thank Somincor/Lundin mining for geochemical data pertaining to the sectors studied. The authors also thank Prof. Elsa Gomes (Coimbra University) and the two anonymous reviewers for their helpful suggestions.

References

Albardeiro, L., Solá, R., Salgueiro, R., Morais, I., Matos, J., Mendes, M., Pereira, Z., Batista, M. J., Inverno, C., Oliveira, D., Rosa, D., Pacheco, N., 2017. Insights into timing of mineralization in the Neves-Corvo VHMS deposit (Iberian Pyrite Belt). Proceedings of the *14th SGA Biennial Meeting – Mineral Deposits to Discover*, August 2017, Québec City, Canada, **3**: 989-992.

Albardeiro, L., Matos, J. X., Mendes, M., Solá, R., Pereira, Z., Morais, I., Salgueiro, R., Pacheco, N., Araújo, V., Oliveira, J. T., 2020. Geological correlation of Neves-Corvo Mine and Pomarão Antiform sequences (Iberian Pyrite Belt, Portugal). *Comunicações Geológicas*, **107**(III): 111-132.

Almodóvar, G. R., Sáez, R., Pons, J. M., Maestre, A., Toscano, M., Pascual, E., 1998. Geology and genesis of the Aznalcóllar massive sulphide deposits, Iberian Pyrite Belt, Spain. *Mineralium Deposita*, **33**: 111-136, https://doi-org-443.webvpn.fjmu.edu.cn/10.1007/978-3-319-17428-0_9

Barrett, T. J., Dawson, G. L., MacLean, W. H., 2008b. Volcanic stratigraphy, alteration, and sea-floor setting of the Paleozoic Feitais Massive Sulfide Deposit, Aljustrel, Portugal. *Economic Geology*, **103**: 215-239. https://doi.org/10.2113/gsecongeo.103.1.215

Barrett, T. J., 2006. *Chemostratigraphy, Petrography and Alteration of Volcanic Rocks at the Lagoa Salgada Deposit, Portugal*. Unpublished report for Redcorp Ventures Ltd., Vancouver. *In:* Redcorp, 2006. Relatório 1º Sem. 1996, Área Lagoa Salgada, Redcorp. LNEG Archive, ID 12379, 33.

Barrett, T., 2004. *Lundin Mining/Somincor geochemical database*. Unpub. Report.

Barrett, T., 2008a. *Chemostratigraphy and petrography of volcanic rocks at the Neves-Corvo deposit, Portugal*. Unpub. Report for Lundin Mining/Somincor, 40.

Barrett, T., 2012. *Lundin Mining/Somincor geochemical database*. Unpub report, 26.

Barrett, T., 2013. *Chemostratigraphy, petrography and alteration of the volcanic rocks at the Lagoa Salgada Deposit, Portugal*. Unpub. Explor. Rep. for Redcorp Ventures, Ltd., LNEG Archive, 17.

Barrett, T., 2014. *Lundin Mining/Somincor geochemical database*. Unpub. Report, 24.

Barrie, C., Amelin, Y., Pascual, E., 2002. U-Pb geochronology of VHMS mineralization in the Iberian Pyrite Belt. *Mineralium Deposita*, **37**: 684-703. https://doi.org/10.1007/s00126-002-0302-7

Barriga, F. J. A. S., Kerrich, R., 1984. Extreme ^{18}O-enriched volcanics and ^{18}O-evolved marine water, Aljustrel, IPB: Transition from high to low Rayleigh number convective regimes. *Geochem Cosmochem Acta*, **48**: 1021-1031. https://doi.org/10.1016/0016-7037(84)90193-5

Barriga, F. J. A. S., Fyfe, W. S., 1988. Giant pyritic base-metal deposits: the example of Feitais (Aljustrel, Portugal). *Chemical Geology*, **69**: 331-343. https://doi.org/10.1016/0009-2541(88)90044-7

Barriga, F. J. A. S., Fyfe, W. S., 1998. Multi-phase water-rhyolite interaction and ore fluid generation at Aljustrel, Portugal. *Mineralium Deposita*, **33**: 188-207. https://doi.org/10.1007/s001260050140

Batista, M. J., Represas, P., Matos, J. X., Inverno, C. M. C., 2014. 3D predictive modelling using drill-hole geochemistry and gravity inversion. First approach using data from Neves-Corvo mining area, Iberian Pyrite Belt, 2014. IX CNG/2º CoGePLiP, Porto, *Comunicações Geológicas*, **101**(II): 747-752. ISSN:0873-948X, e-ISSN: 1647-581X.

Boogaard, M. V. Den., 1963. Conodonts of upper Devonian and lower Carboniferous age from southern Portugal. *Geologie en Minjbouw*, **42**(8): 248-259.

Boogaard, M. V., 1967. *Geology of Pomarão Region (Southern Portugal)*. PhD Thesis, Graffisch Centrum Deltro. Rotherdam, 114.

Carvalho, D., 1971. *Mina de São Domingos. Jazigos Minerais do Sul de Portugal*, Livro-Guia nº4, 59-64.

Carvalho, D., 1976. Considerações sobre o vulcanismo da região de Cercal-Odemira: suas relações com a faixa piritosa. *Comunicações dos Serviços Geológicos de Portugal*, **LX**: 215-238.

Carvalho, D., Barriga, F. J. A. S., Munhá, J., 1999. Bimodal Siliciclastic systems: The case of the Iberian Pyrite Belt. *In:* Barrie, C. T., Hannington, M. D. (Eds.), Volcanic associated massive sulfide deposits: Processes and examples in modern and ancient settings. *Reviews Economic Geology*, 375-408. https://doi.org/10.5382/Rev.08.16

Codeço, M.S.F., 2015. *Estudo comparativo das sequências vulcânicas constituintes dos eixos Ervidel-Roxo e Figueirinha-Albernoa (Faixa Piritosa Ibérica) e respectiva relevância na prospecção de sulfuretos maciços polimetálicos*. Master thesis, Universidade de Lisboa, Portugal, 217.

Codeço, M., Mateus, A., Figueiras, J., Gonçalves, L., Rodrigues, P., 2018. Development of the Ervidel-Roxo and Figueirinha-Albernoa volcanic sequences in Iberian Pyrite Belt, Portugal: metallogenic and geodynamic implications. *Ore Geology Reviews*, **98**: 80-108. https://doi.org/10.1016/j.oregeorev.2018.05.009

Cunha, T., Oliveira, J. T., 1989. Upper Devonian Palynomorphs from the Represa and Phyllite- Quartzite Fm, Mina de São Domingos region, Southwest Portugal. Tectonostratigraphic implications. *Bulletin Société Belge Géologie*, **98**(3/4): 295-309.

Dawson, G. L., Barret, T. J., Caessa, P., Alverca, R., 2001. The Feitais polymetallic massive sulphide deposit, Southern Portugal. *In:* Tornos, F., Pascual, E., Sáez, R., Hidalgo, R. (Eds.), *Massive sulphide deposits in the Iberian Pyrite Belt: new advances and comparison with equivalent systems*. Proceedings of GEODE workshop, *Aracena*, Spain, October 2001. *Geode*, Univ. Huelva, 15.

de Oliveira, D. P. S., Matos, J. X. M., Rosa, C. J. P., Rosa, D. R. N., Figueiredo, M. O., Silva, T. P., Guimarães, F., Carvalho, J. R. S., Pinto, Á. M. M., Relvas, J. R. M. S., Reiser, F. K. M., 2011. The Lagoa Salgada orebody, Iberian Pyrite Belt, Portugal. *Economic Geology*, **106**: 1111-1128. https://doi.org/10.2113/econgeo.106.7.1111

Donaire, T., Pascual, E., Sáez, R., Pin, C., Hamilton, M., Toscano, M., 2020. Geochemical and Nd isotopic signature of felsic volcanic rocks as a proxy of volcanic-hosted massive sulphide deposits in the Iberian Pyrite Belt (SW, Spain): The Paymogo Volcano-Sedimentary Alignment. *Ore Geology Reviews*. **120**: 103408. https://doi.org/10.1016/j.oregeorev.2020.103408.

Elf Aquitaine, 1985. *Recherches pour metaux de premiere classe. Baixo-Alentejo, Portugal.* Unpub. Rep. LNEG Archive.

EPOS, 2014. *Relatório de atividade 2º semestre de 2013*. Contrato Nº MN/PP/049/12 para atribuição de direitos de prospeção e pesquisa de depósitos minerais de ouro, prata, cobre, chumbo, zinco, estanho e metais associados numa área denominada Albernoa situada nos concelhos de Aljustrel, Beja, Mértola e Castro Verde, - à EPOS – Empresa Portuguesa de Obras Subterrâneas, S.A.

Fantinet, D., Dreesen, R., Dusar M., Termier G., 1976. Faunes Famenniennes de certains horizon calcaires dans la formation quartzophylladique aux environs de Mértola (Portugal méridional). *Comunicações dos Serviços Geológicos de Portugal*, **60**: 121-138.

Granado, I., Almeida, J. A., Sousa, J., Carvalho, J., Inverno, C., Rosa, C., Matos, J. X., 2014. Integração de dados e construção de um modelo geológico 3D de uma área a SE na Faixa Piritosa Ibérica, sector Português (Integração de dados num modelo geológico 3D). *Com. Geológicas*, IX CNG/2º CoGePLiP, Porto, **101**(III): 1415-1418. ISSN:0873-948X, eISSN:1647-581X.

Hart, T. R., Gibson, H. L., Lesher, C. M., 2004. Trace element geochemistry and petrogenesis of felsic volcanic rocks associated with volcanogenic massive Cu–Zn–Pb sulfide deposits. *Economic Geology*, **99**: 1003-1013. http://dx.doi.org/10.2113/gsecongeo.99.5.1003

Hughes, C. J., 1973, Spilites, keratophyres, and the igneous spectrum. *Geological Magazine*, **109**: 513-527. https://doi.org/10.1017/S0016756800042795

Inverno, C., 1976. *Rel. Int. sobre cartografia geológica na Mina do Chança*, Serviço de Fomento Mineiro, 8 + 5annexes.

Inverno, C. M. C., Solomon, M., Barton, M. D., Foden, J., 2008. The Cu stockwork and massive sulfide ore of the Feitais volcanic-hosted massive sulfide deposit, Aljustrel, Iberian Pyrite Belt, Portugal: A mineralogical, fluid inclusion, and isotopic investigation: *Economic Geology*, **103**: 241-267. https://doi.org/10.2113/gsecongeo.103.1.241

Inverno, C., Matos, J. X., Rosa, C., Castelo-Branco, J. M., Granado, I., Carvalho, J., Baptista, M. J., Represas, P., Pereira, Z., Oliveira, T., Araújo, V., 2013. Massive sulfide exploration models of the Iberian Pyrite Belt Neves-Corvo mine region, based in a 3D geological, geophysical and geochemical ProMine study. *Geophysical Research Abstracts*, EGU2013-13350-1, European Geosciences Union General Assembly, Viena, *15*.

Inverno, C., Rosa, C., Matos, J., Carvalho, J., Castello-Branco, J. M., Batista, M. J., Granado, I., Oliveira, J. T., Araújo, V., Pereira, Z., Represas, P., Solá, A. R., Sousa, P., 2015. Modelling of the Neves-Corvo Areation and Geological Setting of the Iberian Pyrite Belt. *In*: Weihed, P. (Ed.), *3D, 4D and Predictive Modelling of Major Mineral Belts in Europe*, Springler Verlag, Mineral Resource Reviews, 231-261. DOI 10.1007/978-3-319-17428-0_9.

Ishikawa, Y., Sawaguchi, T., Ywaya, S., Horiuchi, M., 1976. Delineation of prospecting targets for Kuroko deposits based on modes of volcanism of underlying dacite and alteration haloes. *Mining Geology*, **26**: 105-117. https://doi.org/10.11456/shigenchishitsu1951.26.105

Jenner, G. A., 1996. Trace element geochemistry of igneous rocks: Geochemical nomenclature and analytical geochemistry, *In:* Wyman, D. A. (Ed.), *Trace Element Geochemistry of Volcanic Rocks: Applications for Massive Sulfide Exploration*. Geological Association of Canada, Short Course Notes, **12**: 51-77.

Julivert, M., Fontboté, J. M., Ribeiro, A., Conde, L., 1974. *Memoria explicativa del Mapa Tectónico de la Peninsula Ibérica y Baleares, 1/1 000 000*. IGME, Madrid, 1-101.

Large, R. R., McPhie, J., Gemmell, J. B., Herrmann, W., Davidson, G. J., 2001. The spectrum of ore deposit types, volcanic environments, alteration halos, and related exploration vectors in submarine volcanic successions: Some examples from Australia. *Economic Geology*, **96**: 913- 938. http://dx.doi.org/10.2113/96.5.913

Laznicka, P., 1999. Quantitative relationships among giant deposits of metals. *Econ. Geol.* **94**: 455-474. https://doi.org/10.2113/gsecongeo.94.4.455

Leca, X., Ribeiro, A., Oliveira, J. T., Silva, J. B., Albouy, L., Carvalho, P., Merino, H., 1983. Cadre géologique des minéralisations de Neves Corvo (Baixo-Alentejo, Portugal) – Lithostratigraphie, paléogéographie et tectonique. *Mém. BRGM*, **121**: 79.

Leistel, J. M., Marcoux, E., Thiéblemont, D., Quesada, C., Sánchez, A., Ruiz de Almodóvar, G., Pascual, E., Sáez, R., 1998. The volcanic-hosted massive sulphide deposits of the Iberian Pyrite Belt. *Mineralium Deposita*, **33**: 2-30. https://doi.org/10.1007/s001260050130

Leitão, J. C. R., 1992. The Aljustrel overthrust problem in view of thenew evidence from the Sto. Antão area. *Comunicações dos Serviços Geológicos de Portugal*, **78**(2): 97-102.

Leitão, J., 2009. *Geodinâmica varisca, vulcânico-sedimentar e tectónica, na área de Aljustrel*. Tese de Doutoramento, Universidade de Trás-os-Montes e Alto Douro, 448.

Lesher, C. M., Gibson, H. L., Campbell, I. H., 1986. Composition-volume changes during hydrothermal alteration of andesite at Buttercup Hill, Noranda District, Quebec. *Geochimica et Cosmochimica Acta*, **50**: 2693-2705. https://doi.org/10.1016/0016-7037(86)90219-X

MacLean, W. H., Barrett, T. J., 1993. Lithogeochemical techniques using immobile elements. *Journal of Geochemical Exploration*, **48**: 109-133. https://doi.org/10.1016/0375-6742(93)90002-4

MacLean, W. H., Kranidiotis, P., 1987. Immobile elements as monitors of mass transfer in hydrothermal alteration; Phelps Dodge massive sulfide deposit, Matagami, Quebec. *Economic Geology*, **82**: 951-962. https://doi.org/10.2113/gsecongeo.82.4.951

Matos, J. X., Barriga, F. J. A. S., Oliveira, V. M. J., Relvas, J. M. R. S., Conceição, P., 2000. The structure and hydrothermal alteration of the Lagoa Salgada orebody (Iberian Pyrite Belt – Sado Tertiary Basin). *Volcanic Environments and Massive Sulfide Deposits – SEG/CODES International Conf.* Abstract Vol., Tasmania, Australia, 119-121.

Matos, J. X., Filipe, A. (Coord.), 2013. Carta de Ocorrências Mineiras do Alentejo e Algarve à escala 1/400 000, versão digital. Edição LNEG/ATLANTERRA, Lisboa. ISBN: 978-989-675-029-9

Matos, J. X., Oliveira, V., 2003. Mina do Lousal (Faixa Piritosa Ibérica) - Percurso geológico e mineiro pelas cortas e galerias da antiga mina. *IGME, Pub. Museo Geominero*, **2**: 117-128.

Matos, J. X., Pereira, Z., Rosa, C. J. P., Rosa, D. R. N., Oliveira, J. T., Relvas, J. M. R. S., 2011. Late Strunian age: a key time frame for VHMS deposit exploration in the Iberian Pyrite Belt. *11th SGA Biennial Meeting*, Antofagasta, Chile, Abs. Book, **4**: 790-792.

Matos, J. X., Pereira, Z., Rosa, C., Oliveira, J. T., 2014. High resolution stratigraphy of the Phyllite-Quartzite Group in the northwest region of the Iberian Pyrite Belt, Portugal. IX CNG/2º CoGePLiP, Porto, *Comunicações Geológicas*, **101**(I): 489-493. ISSN: 0873-948X, e-ISSN: 1647-581X.

Matos, J. X., Relvas, J. M. R. S., 2006. *Mina do Lousal (Faixa Piritosa Ibérica)*. Livro Guia Excursão C.4.1, VII Cong. Nac. Geologia, Estremoz, U. Évora, Portugal, 23-25.

Matos, J. X., Soares, S., Cardoso, C., 2006. Caracterização Geológica-geotécnica da corta da mina de São Domingos, FPI. *X Cong. Nac. Geotecnia, SPG/UNL*, **3**: 741-752.

Matos, J. X., Rosa, C., 2001. *Diagnóstico Preliminar de Minas Abandonadas – Área Sul*. Rel. Int. IGM, 276.

Mendes, M., Pereira, Z., Matos, J. X., Morais, I., Albardeiro, L., Solá, R., Pacheco, N., Araújo, V., 2018. New preliminary data from Phyllite-Quartzite Formation age based on palynomorphs from Middle-Upper Devonian in Neves-Corvo mine region, Iberian Pyrite Belt (Portugal). *X Congresso Nacional de Geologia, Vulcânica*, **II**: 191-192.

Meschede, M., 1986. A method of discriminating between different types of mid-ocean ridge basalts and continental

tholeiites with the Nb-Zr-Y diagram. *Chemical Geology*, **56**: 207-218, https://doi.org/10.1016/0009-2541(86)90004-5.

Mitjavila, J., Marti, J., Soriano, C., 1997. Magmatic evolution and tectonic setting of the Iberian Pyrite Belt volcanism. *Journal of Petrology*, **38**: 727-755. https://doi.org/10.1093/petroj/38.6.727

Moore, J. G., Hickson, C. J., Calk, L. C., 1995. Tholeiitic–alkali transition at subglacial volcanoes, Tuya region, British Columbia, Canada. *Journal of Geophysical Research*, **100**: 24577-24592. https://doi.org/10.1029/95JB02509

Morais, I., Albardeiro, L., Batista, M. J., Matos, J. X., Mirão, J., Solá, R., de Oliveira, D., Inverno, C., Pacheco, N., Araújo, V., 2019. Hydrothermal alteration of volcanic rocks in the Portuguese sector of the Iberian Pyrite Belt – Application in mineral prospecting – Session GMPV1.1 – Open Session on Geochemistry, Mineralogy, Petrology and Volcanology. *EGU General Assembly*, April, Vienna, Austria, 7-12.

Morais, I., Albardeiro, L., Batista, M. J., Mirão, J., Solá, R., Matos, J. X., Pacheco, N., Araújo, V., Mendes, M., Pereira, Z., Oliveira, D., Salgueiro, R., Marques, F., Inverno, C., 2018a. Geochemical tools for exploration in the Rosário/ Neves-Corvo structure, Iberian Pyrite Belt, Portugal. *XIV Congresso de Geoquímica dos Países de Língua Portuguesa*, 313-317.

Morais, I., Albardeiro, L., Batista, M. J., Mirão, J., Matos, J. X., Pacheco, N., Araújo, V., Solá, R., Salgueiro, R., Oliveira, D., Mendes, M., Pereira, Z., Marques, F., Inverno, C., 2018b. Alteração hidrotermal em metassedimentos na região mineira de Neves-Corvo – Utilização como ferramenta de prospeção mineral. *Revista Portuguesa de Vulcanologia*, X Congresso Nacional de Geologia, **II**: 235-236.

Munhá, J., 1983a. Hercynian magmatism in the Iberian Pyrite Belt. *In:* Sousa, M. J. L., Oliveira, J. T. (Eds.) *The Carboniferous of Portugal*. *Memórias Serviços Geológicos Portugal*, **29**: 39-81.

Munhá, J., 1983b. Low grade metamorphism in the IPB Pyrite. *Com Serv Geol Portugal*, **69**: 3-35.

Oliveira, J. T., 1983. The marine Carboniferous of South Portugal: a stratigraphic and sedimentological approach. *In*: Lemos de Sousa, M. J., Oliveira, J. T. (Eds.), *The Carboniferous of South Portugal*, **29**: 3-38.

Oliveira, J. T., 1990. Stratigraphy and syn-sedimentary tectonism in the South Portuguese Zone. *In:* Dallmeyer, R. D., Martínez-García, E. (Eds.) *Pre-Mesozoic Geology of Iberia* Berlin, Springer-Verlag, 334-347.

Oliveira, J. T., Carvalho, P., Pereira, Z., Pacheco, N., Fernandes, J. P., Korn, D., 1997. Stratigraphy of the Neves Corvo Mine Region. *The Neves Corvo Field Conference - Society of Economic Geology*, 86-87.

Oliveira, J. T., Matos, J. X., 2004. O caminho de ferro da Mina de São Domingos ao Pomarão: um percurso geo-educacional na Faixa Piritosa Ibérica. *XXIV Encontro Prof. Geociências APG*, 19.

Oliveira, J. T., Pereira Z., Carvalho, P., Pacheco, N., Korn, D., 2004. Stratigraphy of the tectonically imbricated lithological succession of the Neves Corvo mine area, Iberian Pyrite Belt, Portugal. *Mineralium Deposita*, **39**: 422-436. https://doi.org/10.1007/s00126-004-0415-2

Oliveira, J. T., Quesada, C., Pereira, P., Matos, J. X., Solá, A. R., Rosa, D., Albardeiro, L., Díez-Montes, A., Morais, I., Inverno, C., Rosa, C., Relvas, J., 2019. South Portuguese Terrane: A Continental Affinity Exotic Unit, Chap. 6. *In:* Quesada, C., Oliveira, T. (Eds.), *The Geology of Iberia: A Geodynamic Approach*. The Variscan Cycle, Regional Geology Reviews, Springer, **2**: 173-206. https://doi.org/10.1007/978-3-030-10519-8_6

Oliveira, J. T., Relvas, J., Pereira, Z., Matos, J., Rosa, C., Rosa, D., Munhá, J. M, Jorge, R., Pino, A., 2006. O Complexo Vulcano-Sedimentar da Faixa Piritosa: estratigrafia, vulcanismo, mineralizações associadas e evolução tectono-estratigráfica no contexto da Zona Sul Portuguesa. *In*: Dias, R., Araújo, A., Terrinha, P., Kullberg, J. C. (Eds.), *Geologia de Portugal no contexto da Ibéria*. Univ. Évora, Évora, 207-243.

Oliveira, J. T., Rosa, C., Rosa, D., Pereira, Z., Matos, J. X., Inverno, C., Andersen, T., 2013. Geology of the Neves-Corvo antiform, Iberian Pyrite Belt, Portugal: New insights from physical volcanology, palynostratigraphy and isotope geochronology studies. *Mineralium Deposita*, **48**: 749-766. https://doi.org/10.1007/s00126-012-0453-0

Oliveira, J., Silva, J., 2007. *Notícia Explicativa da Folha 46-D Mértola da Carta Geológica de Portugal á escala 1/50 000*. Dep. Geologia. INETI, 1-46.

Oliveira, J. T., (Coord.), 1992. Notícia Explicativa da Folha 8 da Carta Geológica de Portugal à escala 1/200 000. *Serviços Geológicos de Portugal*.

Onézime, J., Charvet, J., Faure, M., Bourdier, J. C., Chavet, A., 2003. A new geodynamic interpretation for the South Portuguese Zone (SW Iberia) and the Iberian Pyrite Belt genesis. *Tectonics*, **22**(4): 1-17. https://doi.org/10.1029/2002TC001387

Palme, H., Kleine, T., Rubie, D. C., 2012. Early volatile depletion and rapid core formation in the Earth: Evidence from the 53Mn–53Cr system. *43rd Lunar and Planetary Science Conference*, Abstract #2163.

Paulick, H., Herrmann, W., Gemmell, J. B., 2001. Alteration of felsic volcanics hosting the Thalanga massive sulfide deposit, North Queensland, Australia: Geochemical proximity indicators to ore: *Economic Geology*, **96**: 1175-1200. http://dx.doi.org/10.2113/gsecongeo.96.5.1175

Pearce, J. A., 2008. Geochemical fingerprinting of oceanic basalts with applications to ophiolite classification and the search for Archean oceanic crust. *Lithos*, **100**: 14-48. doi: 10.1016/j.lithos.2007.06.016

Pearce, J. A., Cann, J. R., 1973. Tectonic setting of basic volcanic rocks determined using trace element analyses. *Earth Planet Sci Lett*, **19**(2): 290-300, https://doi.org/10.1016/0012-821X(73)90129-5

Pearce, J. A., Harris, N. B. W., Tindle, A. G., 1984. Trace element discrimination diagrams for the tectonic interpretation of granitic rocks. *J. Petrol*, **25**: 956-983. https://doi.org/10.1093/petrology/25.4.956.

Pearce, J. A., Peate, D. W., 1995. Tectonic implications of the composition of volcanic arc magmas. *Annual Review of Earth and Planetary Sciences*, **23**: 251-285. https://doi.org/10.1146/annurev.ea.23.050195.001343

Pereira *et al*., in press. Geology of the recently discovered Semblana, Rosa Magra and Monte Branco massive and stockwork sulphide deposits, Neves-Corvo mine region, Pyrite Belt, Portugal.

Pereira, Z., Matos, J. X., Batista, M. J., Solá, R., Salgueiro, R., Oliveira, D., Oliveira, J. T., Inverno, C., Rosa, C., 2014. *Caracterização geológica, estratigráfica e litogeoquímica das unidades geológicas da zona do Algaré, Antiforma do Rosário e da mineralização de sulfuretos maciços da Semblana*. Rel. Proj. IPB Vectors, LNEG/Lundin Mining, 150.

Pereira, Z., Matos, J. X., Fernandes, P., Oliveira, J. T., 2008. Palynostratigraphy and Systematic Palynology of the Devonian and Carboniferous Successions of the South Portuguese Zone, Portugal. *Memórias do INETI*, **34**: 1-176.

Pereira, Z., Matos, J. X., Rosa, C., Oliveira, J. T., 2012. Palynostratigraphic importance of the Strunian in the Iberian Pyrite Belt. *45th Annual Meeting AASP and Cimp*, Lexington, KY, USA, 42-43.

Pereira, Z., Matos, J., Fernandes, P., Jorge, R., Oliveira, J. T., 2010. Qual a idade mais antiga da Faixa Piritosa? Nova idade Givetiano inferior para o Grupo Filito-Quartzítico (Anticlinal de S. Francisco da Serra, Faixa Piritosa). *VIII Congresso Nacional de Geologia, E-Terra*, **17**(3): 1-4.

Piercey, S. J., 2009. Lithogeochemistry of volcanic rocks associated with volcanogenic massive sulfide (VHMS) deposits and applications to exploration. *In*: Cousens, B. L., Piercey, S. J. (Eds.) *Subaqeous Volcanism and Mineralization – Modern Through Ancient*. Geological Association of Canada, Short Course Notes, St. John's, NL, Canada, **19**: 15-40.

Piercey, S., 2011. The setting, style and role of magmatism in the formation of volcanogenic massive sulfide deposits. *Mineralium. Deposita*, **46**: 449-471. http://dx.doi. org/10.1007/s00126-011-0341-z

Quesada, C., 1996. Estructura del sector español de la Faja Pirítica: implicaciones para la exploración de yacimientos. *Boletin Geológico y Minero* **107**: 65-78.

Quiring, R., 1936. Die Jungtertiaren Eisenmanganerz-vorkommen in Devon, Karbon und Pliocan vom Sudportugal. Preussichen GeologischenLandsanstalt. Berlin (Arch. Fur Lagerstattenforschung H.63).

Relvas, J., Barriga, F., Bernardino, F., Oliveira, V., Matos, J., 1994. Ore zone hydrothermal alteration in drill hole IGM ± LS1 at Lagoa Salgada, Grândola, Portugal: a first report on pyrophyllyte in a central stockwork. *XIV Reunion Soc Esp Mineral*, Huelva, 150-151.

Relvas, J. M. R. S., Barriga, F. J. A. S., Ferreira, A., Noiva, P. C., Pacheco, N., Barriga, G., 2006. Hydrothermal alteration and mineralization in the Neves-Corvo volcanic-hostemassive sulfide deposit, Portugal. I. Geology, mineralogy, and geochemistry. *Economic Geology*, **101**: 753-790. https://dx.doi.org/10.2113/gsecongeo.101.4.753

Relvas, J. M. R. S., Pinto, A. M. M., Matos, J. X., 2012. Lousal, Portugal: a successful example of rehabilitation of a closed mine in the Iberian Pyrite Belt. *Society for Geology Applied to Mineral Deposits SGA News*, **31**: 1-16.

Relvas, J., Matos, J. X., 2014. Neves-Corvo and the Iberian Pyrite Belt: Facts, questions and future. *Prospectors and Developers Association of Canada Anual Meeting*, Toronto, Canada, Abs.

Rosa, C., McPhie, J., Relvas, J., 2016. Distinguishing peperite from other sediment-matrix igneous breccias: Lessons from the Iberian Pyrite Belt. *Journal of Volcanology and Geothermal Research*, **315**: 8-39. https://10.1016/j.jvolgeores.2016.02.007

Rosa, C. J. P., McPhie, J., Relvas, J. M. R. S., Pereira, Z., Oliveira, T., Pacheco, N., 2008. Facies analyses and volcanic setting of the giant Neves Corvo massive sulfide deposit, Iberian Pyrite Belt, Portugal. *Mineralium Deposita*, **43**: 449-466. https://doi.org/10.1007/s00126-008-0176-4

Rosa, C., Rosa, D., Matos, J., Relvas, J., 2010. The volcanic-sedimentary sequence of the Lousal deposit, Iberian Pyrite Belt (Portugal). *Geophysical Research Abstracts*, EGU 2010, **12**: 2.

Rosa, D. R. N., Inverno, C. M. C., Oliveira, V. M. J., Rosa, C. J. P., 2006. Geochemistry and geothermometry of volcanic rocks from Serra Branca, Iberian Pyrite Belt, Portugal. *Gondwana Research*, **10**: 328-339. https://dx.doi.org/10.1016/j.gr.2006.03.008

Rosa, D. R. N., Inverno, C. M. C., Oliveira, V. M. J., Rosa, C. J. P., 2004. Geochemistry of Volcanic Rocks, Albernoa Area, Iberian Pyrite Belt, Portugal. *International Geology Review*, **46**: 366-383. https://doi.org/10.2747/0020-6814.46.4.366

Rosa, D., Finch, A., Andersen, T., Inverno, C., 2009. U-Pb geochronology and Hf isotope ratios of magmatic zircons from the Iberian Pyrite Belt. *Mineral Petrol*, **95**: 47-69. https://doi.org/10.1007/s00710-008-0022-5

Routhier, P., Aye, F., Boyer, C., Lécolle, M., Molière, P., Picot, P., Roger, G., 1980. La ceinture sud-ibérique à amas sulfurés dans sa partie espagnole médiane, Tableau géologique et métallogénique,Synthèse sur le type amas sulfurés volcano-sédimentaires. *26th Int. Geol. Congr. Paris, Mém BRGM*, **94**: 265.

Sáez, R., Almodóvar, G. R., Pascual, E., 1996. Geological constraints on massive sulphide genesis in the Iberian Pyrite Belt. *Ore Geology views*, **11**: 429-451. https//doi.org/10.1016/S0169-1368(96)00012-1.

Sáez, R., Pascual, E., Toscano, M., Almodóval, G. R., 1999. The Iberian type of volcano-sedimentary massive sulphide deposits. *Mineralium Deposita*, **34**: 549-570. https//doi.org/10.1007/s001260050220

Schermerhorn, L., 1971. An outline stratigraphy of the Iberian Pyrite Belt. *Boletin Geológico y Minero*, España, **82**(3-4): 239-268.

Schermerhorn, L., Staton, W., 1969. Folded overthrusts at Aljustrel (South Portugal). *Geological Magazine*, **106**: 130-141.

Silva, J. B., Oliveira, V., Matos, J., Leitão, J. C., 1997. Field Trip nº2, Aljustrel and Central Iberian Pyrite Belt. *SEG Neves Corvo Field Conference. Guidebook series*, **27**: 73-124.

Silva, J. B., Oliveira, J. T., Ribeiro, A., 1990. South Portuguese Zone Structural outline. *In:* Dallmeyer, R. D., Martinez Garcia, E. (Eds.), *Pre-Mesozoic Geology of Iberia*., Springer Verlag, 348-362.

Solá, R., Albardeiro, L., Salgueiro, R., Morais, I., Díez-Montes, A., Matos, J. X., 2019. Idades U-Pb em rochas vulcano-sedimentares da Zona Sul Portuguesa: resultados preliminares do Projeto GEO-FPI. *Livro de Resumos do XII Congresso Ibérico de Geoquímica – XX Semana da Geoquímica*, 87-90.

Solá, R., Salgueiro, R., Pereira, Z., Matos, J. X., Rosa, C., Araújo, V., Neto, R., Lains, J. A., 2015. Time span of the volcanic setting of the Neves Corvo VHMS deposit. *Cong. Ibérico Geoquímica/XVIII Semana Geoquímica*, 120-123.

Soriano, C., 1997. *Evolucion geodinamica de la Faja Pirítica Ibérica, Zona Sud Portuguesa*. Ph.D. Thesis, Universitat de Barcelona, 328.

Strauss, G. K., 1970. Sobre la geologıa de la provincia piritıfera del Suroeste de la Penınsula Iberica y sus yacimientos, en especial sobre la mina de pirita de Lousal (Portugal). *Memorias del Instituto Geologico y Minero de España*, **77**: 1-266.

Sun, S. S., McDonough, W. F., 1989. Chemical and isotopic systematics of oceanic basalts: implications for mantle composition and processes. *In*: Saunders, A. D., Norry, M. J. (Eds.), *Magmatism in Ocean Basins*, Geological Society of London Special Publications, **42**: 313-345. https://doi.org/10.1144/GSL.SP.1989.042.01.19

Thiéblemont, D., Pascual, E., Stein, G., 1998. Magmatism in the Iberian Pyrite Belt: petrological constraints on a metallogenetic model. *Mineralium Deposita*, **33**: 98-110. https://doi.org/10.1007/s001260050135

Tornos, F., 2006. Environment of formation and styles of volcanogenic massive sulfides: the Iberian Pyrite Belt. *Ore Geology Reviews*, **28**: 259-307. https://doi.org/10.1016/j.oregeorev.2004.12.005

Tornos, F., César, C., Relvas, J. M. R. S., 2005. Transpressional tectonics, lower crust decoupling and intrusion of deep mafic sills: a model for the unusual metallogenesis of SW Iberia. *Ore Geology Reviews*, **27**: 133-163. https://doi.org/10.1016/j.oregeorev.2005.07.020

Tornos, F., López Pamo, E., Sánchez España, F. J., 2008. Iberian Pyrite Belt. *In*: Ángel García-Cortés (Ed.), *Contextos geológicos españoles: una aproximación al patrimonio geológico de relevancia internacional*, Instituto Geológico y Minero de España, Madrid, 56-64.

Walker, R. G., 1979, Turbidites and associated coarse clastic deposits, *In:* Walker, R. G. (Ed.), *Facies Models*, Geoscience Canada Reprint Series, **1**: 91-107.

Webb, J., 1958. Observations on the geology and origin of the San Domingos pyrite deposit. Portugal. *Comunicações dos Serviços Geológicos de Portugal*, **42**: 119-143.

Winchester, J. A., Floyd, P. A., 1977. Geochemical discrimination of different magma series and their differentiation products using immobile elements. *Chemical Geology*, **20**: 325-343, https://doi.org/10.1016/0009-2541(77)90057-2

Wood, D. A., 1980. The application of a Th-Hf-Ta diagram to problems of tectonomagmatic classification and to establishing the nature of crustal contamination of basaltic lavas of the British Tertiary volcanic province. *Earth Planet. Sci. Lett*., **50**(1): 11-30, https://doi.org/10.1016/0012-821X(80)90116-8